TECHNISCHE UNIVERSITÄT MÜNCHEN

Fakultät für Medizin

Txnrd2 deficiency inhibits Epithelial-to-Mesenchymal-Transition (EMT) in pancreatic ductal adenocarcinoma (PDAC)

Chao Wu

Vollständiger Abdruck der von der Fakultät für Medizin der Technischen Universität München zur Erlangung des akademischen Grades eines

Doktors der Medizin (Dr. med.)

genehmigten Dissertation.

Vorsitz: apl. Prof. Dr. Bernhard Haslinger

Prüfer der Dissertation:

1. Prof. Dr. Roland M. Schmid

2. apl. Prof. Dr. Dr. Ihsan Ekin Demir

Die Dissertation wurde am 26.01.2023 bei der Fakultät für Medizin der Technischen Universität München eingereicht und durch die Fakultät für Medizin am 18.07.2023 angenommen.

TABLE OF CONTENTS

LIST OF ABBREVIATIONS

ADP	adenosine diphosphate
AMPK	AMP-activated protein kinase
AP-1	activating protein-1
ATM	ATM serine/threonine kinase,
ATP	adenosine triphosphate
BMI	body mass index
BRCA1/2	breast cancer type 1/2
CDKN2A	cyclin Dependent Kinase Inhibitor 2A
DHODH	dihydroorotate dehydrogenase
DOX	doxycycline
E-CADHERIN	epithelial cadherin
EMT	epithelial-mesenchymal transition
EMT-TFs	epithelial-mesenchymal transition transcription factors
FBS	Fetal Bovine Serum
GPDH	glycerol-3-phosphate dehydrogenase
GPX8	glutathione Peroxidase 8
GSH	glutathione
GSST2	glutathione s-transferase theta 2
HIF-1α	hypoxia-inducible factor 1-alpha
HSF1	heat Shock Transcription Factor 1
MAOs	monoamine oxidases
mTOR	mammalian target of rapamycin
N-CADHERIN	neural cadherin

NF-κB	nuclear factor kappa-light-chain-enhancer of activated B cells
NRF2	the nuclear factor erythroid 2–related factor 2
PDAC	pancreatic ductal adenocarcinoma
PRDX1	peroxiredoxin 1
PRDX2	peroxiredoxin 2
PRRX1a/b	paired related homeobox 1a/b
Prx3	peroxiredoxin 3
RNS	reactive nitrogen species
ROS	reactive oxygen species
SNAI2	zinc finger protein SNAI2
SNAI1	zinc finger protein SNAI1
SOD	superoxide dismutase
TP53	tumor protein P53
TRX	thioredoxin
TWIST	twist family BHLH transcription factor
TXNRD1	thioredoxin reductase 1
TXNRD2	thioredoxin reductase 2
β-CATENIN	catenin beta-1

LIST OF TABLES

LIST OF FIGURES

ABSTRACT

Pancreatic ductal adenocarcinoma (PDAC) is the predominant form (around 90%) of pancreatic malignancies. PDAC ranks fourth place in causes of cancer-related deaths in the world. Accumulating evidence shows that epithelial-mesenchymal transition (EMT) is one of the reasons for PDAC poor prognosis. Of note, the expression of EMT-transcription factors (EMT-TFs), such as zinc finger protein SNAI1/2 (SNAI1/2), twist family BHLH transcription factor 1/2 (TWIST1/,2) and Zinc finger E-box-binding homeobox 1/2 (ZEB1/2), are controlled by transcription factors activated by reactive oxygen species (ROS).

In our study, it was identified that thioredoxin reductase 2 (Txnrd2), a member of the thioredoxin (TRX) system in regulating balance of redox in cells, was up-regulated in CK-MES cells compared to CK-EPI cells. Pharmacological repression of Txnrd2 by Auranofin inhibited EMT in pancreatic cancer cells. The colony formation capacity and cell proliferation were also inhibited after Txnrd2 was repressed by Auranofin. In addition, Txnrd2 shows the influence on AMP-activated protein kinase (AMPK) signaling pathway that AMPK was activated when Txnrd2 was repressed by Auranofin. Furthermore, EMT, cell proliferation and colony formation capacity were inhibited after *Txnrd2* was knocked down genetically in CK-MES cells. Similarly, AMPK was activated after *Txnrd2* was knocked down. In addition, the primary *Txnrd2*-deficient cells were obtained by isolating from the LSL-*Kras*$^{G12D/+}$; *Ptf1a*$^{Cre/+}$; *Txnrd2*$^{fl/fl}$ mice, and restored Txnrd2 expression by introducing an inducible *Txnrd2* vector into those cells. Loss of *Txnrd2* led to activation of AMPK. EMT was repressed in *Txnrd2*-deficient cells. However, the above effects were reversed via Txnrd2 rescuing by treating cells with Doxycycline (DOX).

In conclusion, Txnrd2 is positively associated with mesenchymal phenotype in pancreatic cancer. Cell proliferation, colony formation capacity, and EMT are repressed when Txnrd2 is pharmacologically inhibited or genetically knocked down. As a regulator of redox balance, repression of Txnrd2 activates AMPK pathway which may also retard EMT in pancreatic cancer.

ZUSAMMENFASSUNG

Das duktale Adenokarzinom des Pankreas (PDAC) ist eine vorherrschende Form (etwa 90 %) der malignen Erkrankungen der Bauchspeicheldrüse. PDAC belegt weltweit den vierten Platz bei den krebsbedingten Todesursachen. Immer mehr Beweise zeigen, dass die epithelial-mesenchymale Transition (EMT) einer der Gründe für die schlechte Prognose von PDAC ist. Bemerkenswert ist die Expression von EMT-Transkriptionsfaktoren (EMT-TFs), wie z. bindende Homöobox 1/2 (ZEB1/2), werden durch Transkriptionsfaktoren kontrolliert, die durch reaktive Sauerstoffspezies (ROS) aktiviert werden.

In unserer Studie haben wir festgestellt, dass Txnrd2, ein Mitglied des Thioredoxin (TRX)-Systems bei der Regulierung des Redox-Gleichgewichts in Zellen, in CK-MES-Zellen im Vergleich zu CK-EPI-Zellen hochreguliert war. Die pharmakologische Repression von Txnrd2 durch Auranofin hemmte die EMT in Bauchspeicheldrüsenkrebszellen. Die Fähigkeit zur Koloniebildung und Zellproliferation wurde ebenfalls gehemmt, während Txnrd2 durch Auranofin reprimiert wurde. Darüber hinaus zeigt Txnrd2 einen Einfluss auf den AMPK-Signalweg, indem AMPK aktiviert, wenn Txnrd2 durch Auranofin reprimiert wurde. Darüber hinaus wurden EMT, Zellproliferation und Koloniebildungskapazität gehemmt, nachdem Txnrd2 in CK-MES-Zellen genetisch ausgeschaltet wurde. In ähnlicher Weise wurde AMPK aktiviert nachdem Txnrd2 niedergeschlagen wurde. Darüber hinaus erhielten wir primäre *Txnrd2*-defiziente Zellen, die aus LSL-*Kras*$^{G12D/+}$ isoliert wurden; *Ptf1a*$^{Cre/+}$; *Txnrd2*$^{fl/fl}$-Mäuse und stellten die Txnrd2-Expression durch Einführen eines induzierbaren *Txnrd2*-Vektors in diese Zellen wieder her. Offensichtlich führte der Verlust von Txnrd2 zur Aktivierung von AMPK. EMT wurde in Txnrd2-defizienten Zellen unterdrückt. Der obige Effekt wurde jedoch über die Txnrd2-Rettung durch die Behandlung von Zellen mit DOX umgekehrt.

Zusammenfassend ist Txnrd2 positiv mit dem mesenchymalen Phänotyp bei Bauchspeicheldrüsenkrebs assoziiert. Zellproliferation, Koloniebildungskapazität und EMT werden unterdrückt, wenn Txnrd2 pharmakologisch gehemmt oder genetisch ausgeschaltet wird. Als Regulator des Redoxgleichgewichts aktiviert die Unterdrückung von Txnrd2 den AMPK-Weg, der auch zur Verzögerung der EMT bei Bauchspeicheldrüsenkrebs beitragen kann.

I. INTRODUCTION

I.1. PANCREATIC CANCER

Pancreatic cancer has an inferior prognosis accompanied by increased incidence and high mortality (Siegel et al., 2014). There are several factors that contribute to low survival rate and late diagnosis is considered as the most important factor leading to poor prognosis (Gillen et al., 2010). The global burden of pancreatic cancer continuously increased over the past two decades (Collaborators, 2019). The increasing prevalence of major risk factors, especially in high-income countries, has caused an age-adjusted increase in pancreatic cancer incidence. The age-standardized incidence rate has increased from 5.0 per 100,000 person-years in 1990 to 5.7 per 100,000 person-years in 2017 (Collaborators, 2019). Figure I.1 shows incidence rates are generally high in North America, Europe, and Argentina, followed by East Asia and Australia. Furthermore, in the United States, age-adjusted incidence rates in 2017 were higher among black individuals (15.9 per 100,000 person-years) than among whites (13.4 per 100,000 person-years) and SEER-defined Hispanic individuals (11.7 per 100,000 person-years) and Asians (10.2 per 100,000 person-years) (Collaborators, 2019; Klein, 2021). A projection study points out that pancreatic cancer may become the fifth most common cancer and rank the second most common cause of cancer-related deaths in Germany by the year of 2030 (Quante et al., 2016). Globally, the incidence of pancreatic cancer tends to be slightly higher in men than in women, especially in those under the age of 75 (Collaborators, 2019).

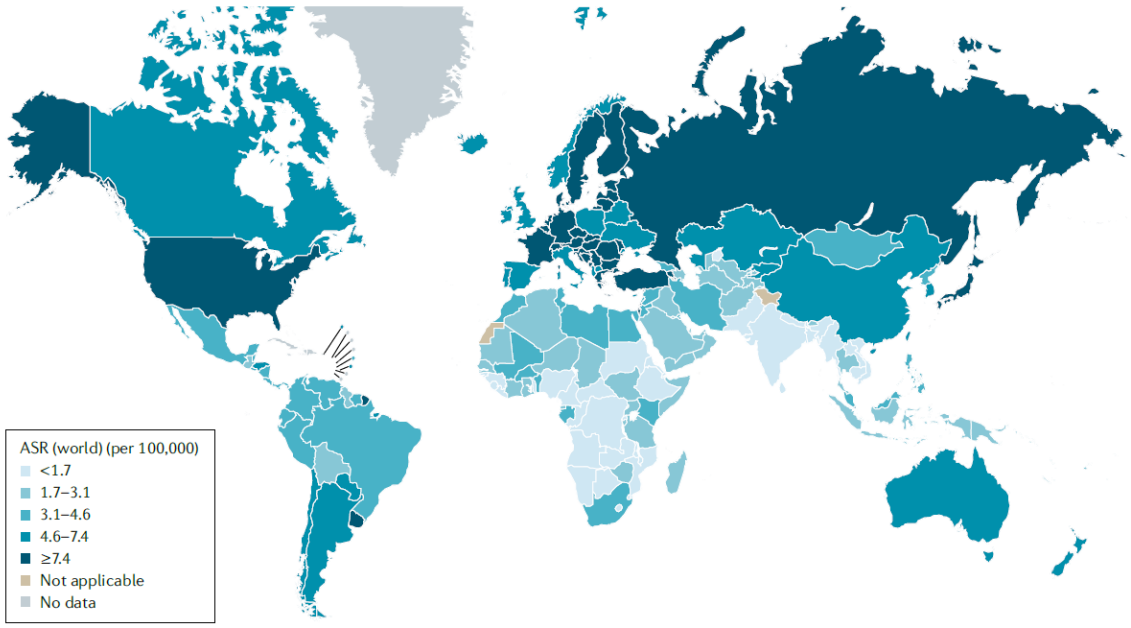

Figure I.1. The incidence of pancreatic cancer in the world. Different colors represent the age-standardized incidence rates (ASR) of pancreatic cancer in each country in 2020. The data was obtained from International Agency for Research on Cancer (accessed 14 April 2021). Legend was modified and picture was taken from Reference (Klein, 2021).

Pancreatic cancer survival rate remains low despite the improvements that have been achieved in recent years. The 5-year overall survival rate is from less than 5% in the 1990s slightly increasing to 9% in the US and Europe in 2019 (Jemal et al., 2006; Siegel et al., 2020). Poor survival is mostly due to the advanced stage at diagnosis. Only about 20% of patients are diagnosed at early-stage that have the chance to be surgically resected. Among the patients with surgical resection, the overall 5-year survival rate is 15-25%, while patients in stage 1A show a higher survival rate of over 80% in the United States (Blackford et al., 2020; He et al., 2014). The majority of pancreatic cancers is pancreatic ductal adenocarcinoma that accounts for more than 90% in all pancreatic cancer cases (Wood & Hruban, 2012).

Pancreatic cancers arise from both the exocrine and endocrine parenchyma of the gland. Around 95% of pancreatic cancers arise from ductal epithelium, acinar cells or connective tissue and occur with the exocrine portion. Ductal adenocarcinoma is the most common pancreatic cancer. There are variant ductal carcinoma with different morphorlogies, such as colloid carcinoma and medullary carcinoma. Adenosquamous carcinoma and undifferentiated carcinomas with osteoclast-like giant cells are associated with poorer prognosis, whereas acinar cell pancreatic cancers have a better prognosis (Ducreux et al., 2015; Wisnoski et al., 2008).

Current studies have illustrated several risk factors that may lead to pancreatic cancers:

Cigarette smoking

Smoking is a known risk factor of pancreatic cancer (Bosetti et al., 2012; Iodice et al., 2008; Lynch et al., 2009). In a meta-analysis of smoking as pancreatic cancer risk, the odds ratio is 1.74 (95% CI 1.61-1.87) for current smokers compared with never-smokers. The risk is positively associated with the amount of cigarette consumption. Smoking cessation reduces this risk, with an odds ratio of 1.2 (95% CI 1.11-1.29) for pancreatic cancer among ex-smokers compared to never-smokers (Iodice et al., 2008).

Diabetes mellitus

Diabetes mellitus is both a risk factor and a consequence of pancreatic cancer (Bosetti et al., 2014; Elena et al., 2013; Everhart & Wright, 1995; Huxley et al., 2005). Many

patients with newly diagnosed pancreatic cancer are observed with either developing diabetes or aggravated diabetes. Interestingly, recent diagnosed diabetes less than 4 years has a higher risk of the malignant pancreatic cancer compared to the long-term diabetes over 5 years (Huxley et al., 2005). However, the association between pancreatic cancer and diabetes over 9 years is weak (Elena et al., 2013; Li et al., 2011).

Body mass index

Increased body mass index (BMI) has been shown to increase the risk of pancreatic cancer. Using data from the Health Professional Follow-up and Nurses' Health Survey of 46,648 men and 117,041 women in the United States in 2001, Michaud et al. estimated the subjects' relative risk of pancreatic cancer is 1.72 (95% CI 1.19 –2.4) after accounting for the effects of age, smoking, and diabetes, subjects with a BMI > 30 kg/m^2 compared with those with a BMI < 23 kg/m^2 (Michaud et al., 2001).

Pancreatitis

Pancreatitis, like diabetes, is a risk factor for pancreatic cancer. The inflammation and correlated damages lead to the development of pancreatic cancer. However, studies point out that pancreatitis can develop as a result of pancreatic cancer in some cases (Yadav & Lowenfels, 2013). A pooled analysis within the PanC4 consortium shows that 6% of 4,444 patients with pancreatic cancer reported a history of pancreatitis compared to 1% in the control group. The odds ratio for pancreatitis with a recent diagnosis of pancreatic cancer is 2.71 (95% CI 1.96-3.74), indicating an association between pancreatitis and pancreatic cancer (Duell et al., 2012).

Microbiota

Over the past decade, scientists gained interest in the role of the microbiota in pancreatic cancer (Riquelme et al., 2019). A meta-analysis shows that periodontitis and tooth loss is associated with a 50-70% increased risk of pancreatic cancer (Maisonneuve et al., 2017). Oral microbiota, specifically *Porphyromonas gingivalis* and *Aggregatibacter actinomycetemcomitans*, are correlated to the development of pancreatic cancer in 361 individuals, according to the American Cancer Society Cancer Prevention Study (Fan et al., 2018). These bacterial species are also associated with future risk of lung, colorectal, and ovarian cancer (Fan et al., 2018).

Pancreatic ductal adenocarcinoma (PDAC)

Pancreatic ductal adenocarcinoma (PDAC) accounts for approximately 90% of all pancreatic malignancies (Kleeff et al., 2016). PDAC ranks fourth in causes of cancer-related deaths worldwide and the 5-year overall survival rate of PDAC is less than 8% (Siegel et al., 2018). Obesity and type 2 diabetes are two implications of PDAC etiology (Calle et al., 2003; Font-Burgada et al., 2016; Rahn et al., 2018). Other risk factors, such as alcohol and tobacco, are also involved in PDAC development (Delitto et al., 2016; Gapstur et al., 2011; Olson et al., 2010; Pelucchi et al., 2014; S. Zhang et al., 2017). Approximately 90% of PDACs habor the mutation of *KRAS.* In addition, the mutant alleles of *KRAS* are amplified in a subgroup of samples, promoting tumour progression. Mutation of *KRAS* impairs the hydrolyzation of GTP, which activates downstream signaling pathways subsequently driving cell proliferation (Mann et al., 2016). Mutation in the codon 12 of *KRAS* is most frequent in PDACs. The point

mutation results in a single amino acid substitution of glycine by aspartic acid (G12D), valine (G12V), arginine (G12R), alanine (G12A) or cysteine (G12C). G12D mutation accounts for 45% in all types of mutations in PDACs (Moore et al., 2020). *KRAS* mutations are observed at the earliest stage of PDAC development (PanIN1) (Kanda et al., 2012), which implies that *KRAS* mutation is critical for tumor initiation. Furthermore, some studies validated that mutant *KRAS* signaling is required at the later stage of PDAC development (Collins et al., 2012). Germline mutations of *BRCA1 DNA repair associated/ BRCA2 DNA repair associated* (*BRCA1/2*), *ataxia-telangiectasia mutated* (*ATM*), *tumor protein p53* (*TP53*) or *cyclin-dependent kinase inhibitor 2A* (*CDKN2A*) are typical genetic alterations that account 5-6% of all PDAC patients (Hu et al., 2018; Petersen et al., 2010; Pihlak et al., 2017). The multi-step of PDAC development is shown and explained in Figure I.2.

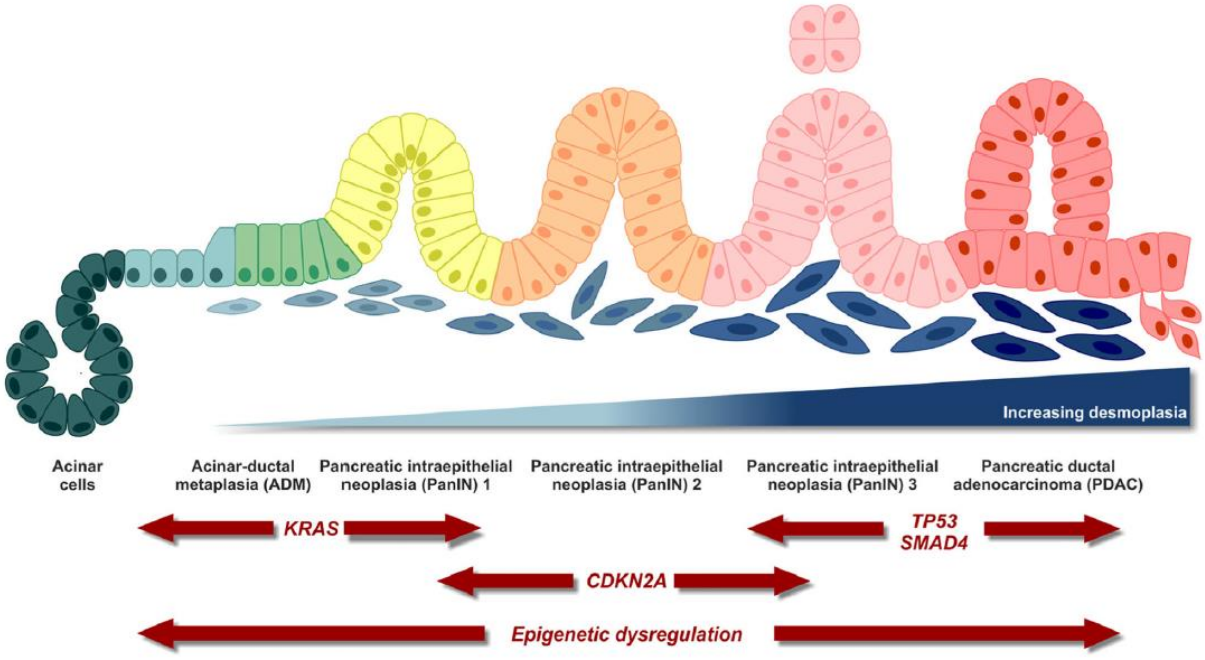

Figure I.2. Multi-step PDAC carcinogenesis. The pancreas consists of acinar, ductal and endocrine cells. High plasticity is the main feature of acinar cells, which drives the homeostasis and regeneration of the pancreas. Certain macro- or microenvironment stimulates acinar cells to undergo transdifferentiation to ductal-like phenotype, called

acinar-to-ductal metaplasia (ADM). *KRAS* mutations promote the transformation of ADM to pancreatic intra-epithelial neoplasias (PanINs). PDAC also contains other mutations or expression alterations of *TP53*, *CDKN2A* and *SMAD4*. (Orth et al., 2019)

Metastasis is one of the main features of PDAC (Kleeff et al., 2016). The distal invasion is observed in other gastrointestinal organs as well as in the vascular and nervous system in some cases (Poruk et al., 2013). The metastasis of PDAC originates from a few disseminated tumor cells with high metastatic potential (Campbell et al., 2010; Makohon-Moore et al., 2017). Epithelial-to-mesenchymal transition (EMT) is the first step of metastasis that multiple signals promote the transdifferentiation of epithelial cells into motile mesenchymal cells (Lamouille et al., 2014). The process induces cancer progression. Studies have shown that EMT partly explains the metastasis of PDAC (Collisson et al., 2011; Moffitt et al., 2015; Rhim et al., 2012). Deregulation of mesenchymal genes including *TWIST1/2*, *SNAI1/2*, *ZEB1/2* and *PRRX1a/b* promotes PDAC metastasis, which results in a poor prognosis (Takano et al., 2016; Wang et al., 2017). MicroRNAs also constitute EMT in PDAC by repressing the expression of EMT associated genes (Giovannetti et al., 2017; Mees et al., 2010). PDAC EMT and metastasis formation are shown in Fig I.3.

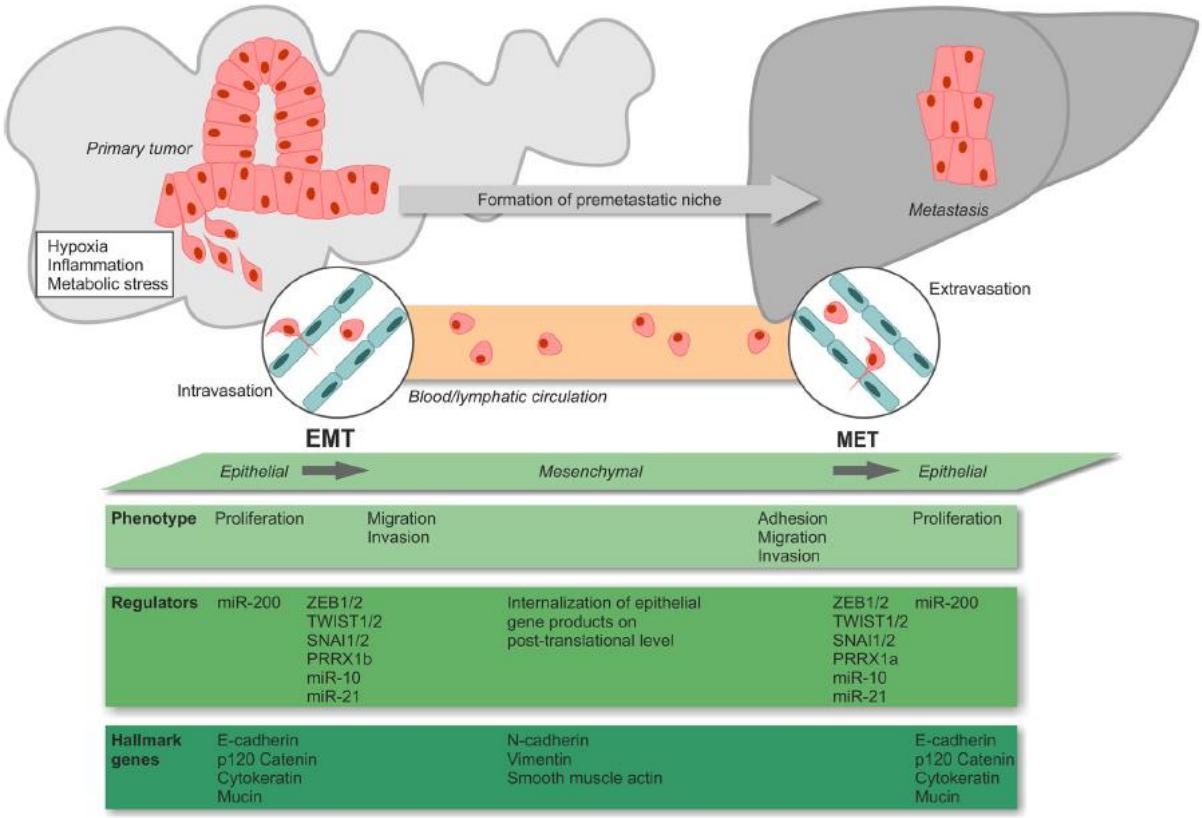

Figure I.3. PDAC epithelial-mesenchymal transition and metastasis formation. Enhanced metastasis formation causes the poor prognosis of the quasi-mesenchymal PDAC subtype with deregulated mesenchymal genes. Quasi-mesenchymal PDAC subtype is designated by Collisson *et al* according to the interpretation of specific gene expression. High expression of mesenchyme-associated genes is the main feature of this subtype (Collisson et al., 2011). Picture was taken from reference (Orth et al., 2019). EMT, epithelial-to-mesenchymal transition; MET: mesenchymal-to-epithelial transition.

I.2. EPITHELIAL-TO-MESENCHYMAL TRANSITION (EMT) AND PDAC

I.2.1. EMT AND CANCER

During embryonic development, tissue repair, and tumorigenesis, EMT occurs as a transient and reversible transdifferentiation program (Hay, 2005; Kalluri & Weinberg, 2009; Nieto et al., 2016; Palamaris et al., 2021; Shook & Keller, 2003). The epithelial-mesenchymal axis is characterized by multiple genetic and epigenetic alterations that occur in a stepwise manner. SNAI1/2, TWIST1/2, and ZEB1/2 are transcription factors responsible for regulating EMT in cells (Peinado et al., 2007). The pleiotropic nature of these transcription factors represses epithelial features and activates mesenchymal features in order to progressively alter cellular physiology. EMT transcriptional program induces several key molecular switches, including cytoskeletal remodeling by replacing epithelial cytokeratins with mesenchymal intermediate filament vimentin, loosening of intercellular junctions between adjacent cells, partial repression of E-cadherin and activation of N-cadherin, and inducing matrix-metalloproteinase expression (Lamouille et al., 2014). Multiple phenotypic features of epithelial cells alter as a result of widespread reprogramming of gene expression profile, which leads to changes in cell morphology from squamous, cuboidal or columnar to spindle-like forms as well as loss of apical-basal polarity and a concomitant increase in front-rear polarity (Palamaris et al., 2021). EMT drives the acquisition of mesenchymal features thereby paving the way for cancer cells to complete multiple steps of metastasis. Interestingly, EMT is associated with the rewiring of energy consumption in cancer cells (Li & Li, 2015).

I.2.2. EMT AND PDAC

Accumulating evidence shows that EMT is one of the reasons for PDAC poor prognosis. The expression of EMT-TFs is altered in resected PDAC specimens compared to surrounding parenchyma (Hotz et al., 2007). A retrospective study

revealed that high level of EMT-TFs is positively correlated to the presence of lymph node metastasis in 174 PDAC patients (Yamada et al., 2013). EMT also appears to be associated with tumor budding and a high risk of mortality and recurrence (Chouat et al., 2018; Galvan et al., 2015; Kohler et al., 2015; Lapshyn et al., 2017; Lawlor et al., 2019; Liu et al., 2017; Wartenberg et al., 2018). In the early stage of pancreatic cancer dissemination, EMT occurs in pre-cancerous lesions of PDAC that enables cells to disseminate to adjacent stroma from the ductal structures (Figure I.4).

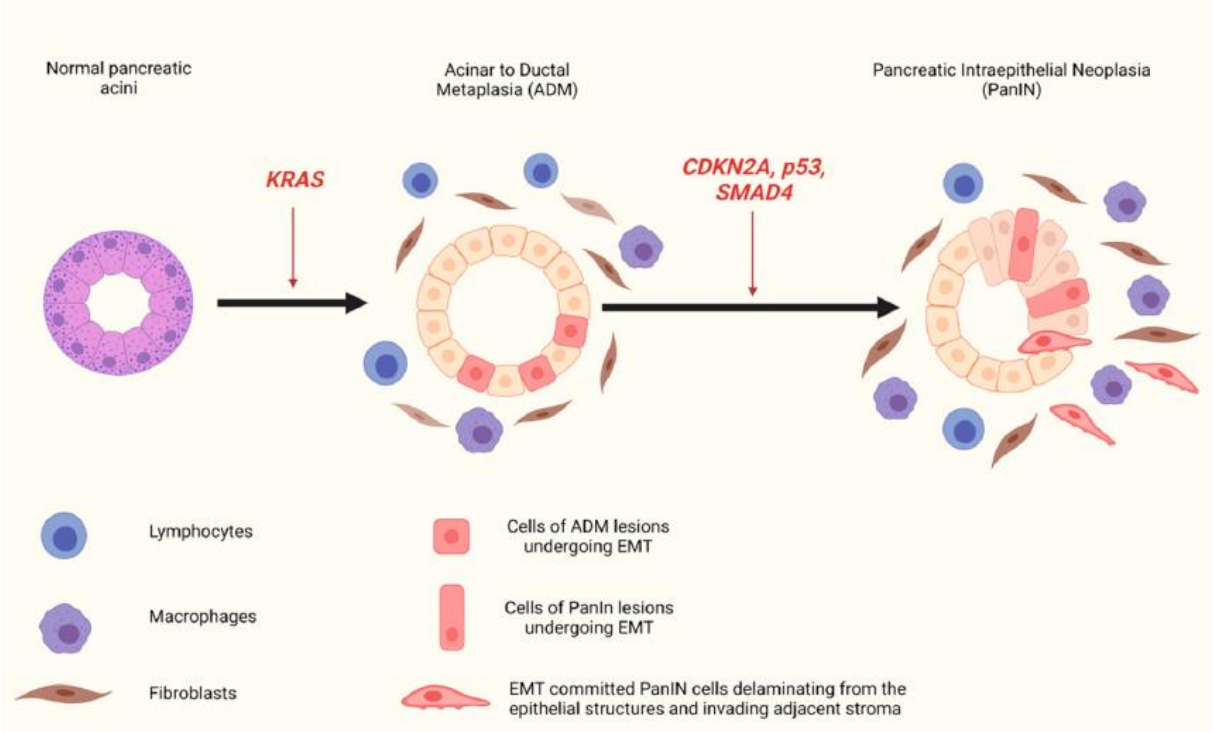

Figure I.4 EMT and early dissemination of pancreatic cancer. The inflammatory microenvironment is a major cause that drives EMT in pre-cancerous lesions of pancreatic ductal adenocarcinoma. In this case, many cells within acinar-to-ductal metaplasia and PanIN lesions undergo EMT. In the initial stage of invasion tumor, EMT-committed cells escape from the ductal structures and disseminate to the adjacent stroma with high invasion ability. Picture was taken from (Palamaris et al., 2021).

The mutation of *KRAS* has been identified by multiple studies in the initiation and maintenance of PDAC. Approximately 90% of PDACs show *KRAS* mutation and most mutations happen at amino acid position 12 where a single glycine is replaced by aspartic acid , namely $KRAS^{G12D}$ (Hobbs et al., 2016). With this mutation, the activity of KRAS is abnormally increased due to the prevention of the interaction between KRAS and GTPase activating proteins (GAPs) (Rozengurt & Eibl, 2021). Nevertheless, other activated or inactivated signaling pathways mediated by additional mutations are also required for PDAC development. Inactivation of *CDKN2A* paves the way for PDAC EMT in the early steps. Inactivation of *p53* and *SMAD4* mediates the following steps of PDAC metastasis in late stages (Rozengurt & Eibl, 2021). Moreover, it has been shown that *p53* is the only predominant tumor suppressor undergoing missense mutation in PDAC development rather than the loss of function of as in the case of *CDKN2A* and *SMAD4* (Kim et al., 2021).

Furthermore, SMAD4 can directly induce the transcription of *ZEB1*, *SNAI1* and *FOS like 1* (*FOSL1*) (Ahmed et al., 2017; Dai et al., 2021). Therefore, transforming growth factor β (TGFβ) appears to be a key promoter of EMT in PDAC, which is mediated by SMAD4 (Kang et al., 2014). In addition to the regulation of EMT inducer genes, TGFβ/SMAD4 signaling is involved in increased expression of vascular endothelial growth factor (VEGF), epidermal growth factor receptor (EGFR), and the stemness marker CD133 (Chen et al., 2014).

Currently, there are two cellular models to depict the metastasis of PDAC. The first classic model suggests that metastasis is the result of a “Darwinian” evolutionary process. Metastatic competent clones are selected by pressure after rounds of genetic or epigenetic changes in primary tumor (Cairns, 1975; Palamaris et al., 2021). The

second model favors metastasis as an inherent property of tumors generated early in their natural history (Hellman, 1994; Klein, 2009; Palamaris et al., 2021). Many *in vivo* studies support the second model as genetically engineered PDAC mouse strains are generated based on simultaneous conditional *Kras* gain-of-function mutation and *p53* (Hingorani et al., 2005) or *p16* (Aguirre et al., 2003) deletion. Studies have shown that EMT in PDAC is induced by different paracrine factors and multiple signaling pathways: cytokines, growth factors and DNA damage response pathways contribute to the reprogram of EMT in PDAC (Figure I.5).

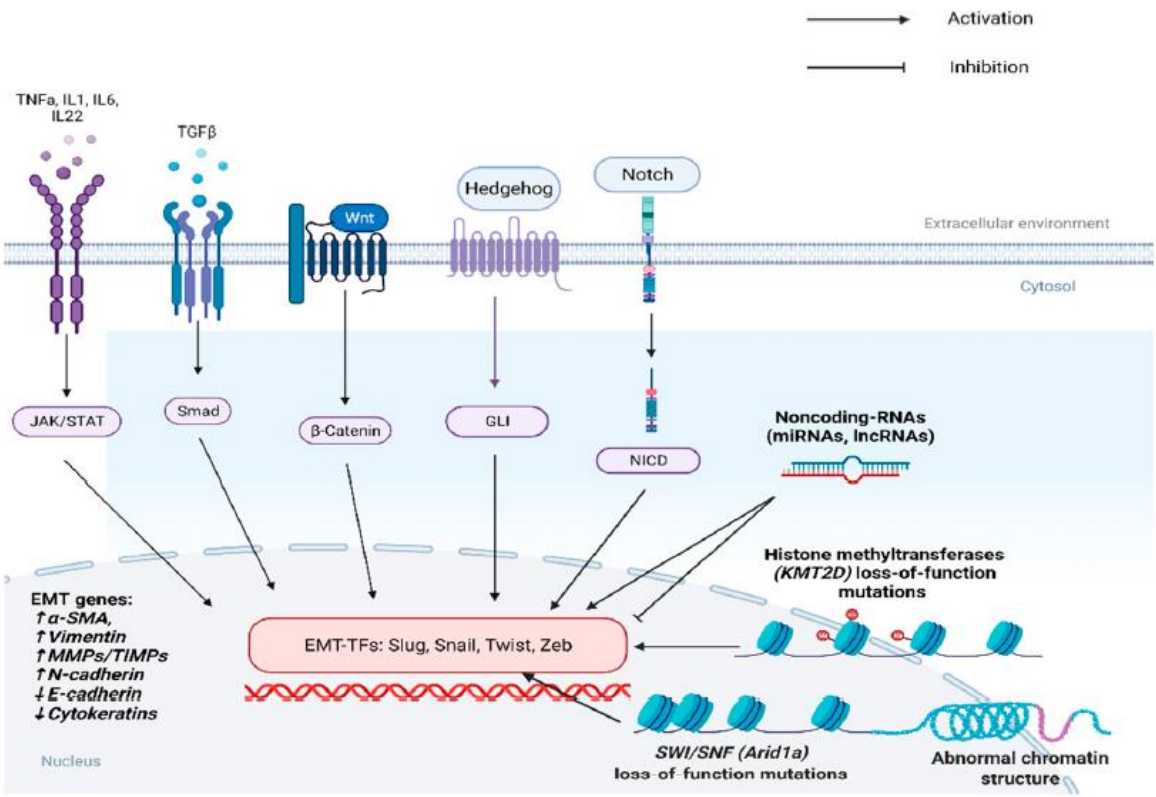

Figure I.5. EMT is controlled by a variety of signaling pathways and epigenetics factors, including histone methyltransferases, chromatin remodeling complexes, and non-coding RNAs in PDAC. The picture was taken from (Palamaris et al., 2021). a-SMA: alpha Smooth Muscle Actin, MMPs: Matrix Metalloproteinases, TIMPs: Tissue Inhibitors of Metalloproteinases.

I.3. Oxidative stress and cancer

Oxidative stress is associated with a variety of diseases including neurodegenerative disease, cardiovascular disease and diabetes mellitus (Sies, 2015). The imbalance of reactive oxygen species (ROS) and antioxidants results in oxidative stress, which perturbs a variety of proteins involved in molecular pathways, such as c-MYC, p53, protein kinase C (PKC) and nuclear factor erythroid 2-related factor 2 (NRF2) (Martinez-Useros et al., 2017). Increased ROS has been identified in cancers that triggers pathways to promote tumorigenesis and cell survival. The phosphatidylinositol-3 kinase/protein kinase B (PI3K-Akt) pathway is induced by ROS via repressing phosphatase and tensin homolog (PTEN) (Koundouros & Poulogiannis, 2018).

The redox homeostasis is usually aberrant in cancer cells. Interestingly, mild ROS promotes tumor progression, whereas a high level of ROS is cytotoxic (Reczek et al., 2017). Tumor cells with high proliferative capacity are commonly accompanied by high ROS production. To avoid cellular senescence, apoptosis or ferrotosis, cancer cells can increase the production of antioxidants to alleviate oxidative stress, thereby optimizing ROS-driven proliferation (Dodson et al., 2019; Redza-Dutordoir & Averill-Bates, 2016).

ROS and reactive nitrogen species (RNS) are consequences of cell metabolism and they serve as intracellular signaling molecules in tumorigenesis (Hayes et al., 2020). To avoid damage caused by ROS/RNS induced oxidative stress, cells acquire a system of antioxidants that induce detoxification of reactive metabolites and the

formation of ROS/RNS (Hayes et al., 2020). In addition, the transcriptional program changes when cells face long-term or chronic oxidative stress (Hayes et al., 2020).

Current studies indicate that many transcription factors are involved in the adaptation to oxidative stress. Activator protein 1 (AP-1), hypoxia inducible factor 1 subunit alpha (HIF-1α), heat shock transcription factor 1 (HSF1), nuclear factor kappa B subunit 1 (NF-Kb), NRF2 and p53 are all activated by ROS and participate in the regulation of redox status (Marinho et al., 2014). Interestingly, it seems that different transcription factors respond to distinct threshold levels of ROS/RNS. Typically, NRF2 is considered as a first-tier defense in response to oxidative stress. When higher ROS/RNS level appears, AP-1 and NF-κB are activated as the second-tier defense. Apoptosis is the final tier in extremely high ROS/RNS levels (Xiao et al., 2003).

Mitochondria are the main source of ROS that are by-products of the oxidative phosphorylation (OXPHOS) (Chandra & Singh, 2011). Aberrant electron transport chain impairs the function of mitochondria, which decreases OXPHOS and induces mitochondrial ROS (mtROS) and oxidative stress (Chandra & Singh, 2011).

Of note, the expression of EMT-TFs is controlled by transcription factors activated by ROS. For example, AP-1, HIF-1α, HSF1, NF-κB and p53 regulate the expression of SNAI1/2, TWIST1/2 and ZEB1/2 (Jiang et al., 2017). Therefore, the deregulated redox could trigger EMT and promotes tumor progression.

I.4. AMPK PATHWAY

5'-AMP-activated protein kinase (AMPK) is a heterotrimeric Ser/Thr kinase complex with one catalytic subunit and two regulatory subunits (Zadra et al., 2015). AMPK is a

sensor that restores energy homeostasis in the condition of metabolic stress. Activation of AMPK triggers metabolic adaptation and maintains ATP and NADPH levels, which is required for cell survival (Hardie et al., 2012). Deregulation of AMPK impairs the balance of redox homeostasis and results in metabolic diseases and cancer. LKB1-STRAD-MO25 complex (Hawley et al., 2003; Shaw et al., 2004; Woods et al., 2003) and Ca^{2+}/calmodulin-activated protein kinase kinase (CaMKKs) (Hawley et al., 2005; Hurley et al., 2005; Woods et al., 2005) activate AMPK as up-stream kinases. In mammalian cells, AMPK is activated by multiple factors including metabolic stress and xenobiotics through mentioned kinases above, which refers as the classical or canonical AMPK activation. Increasingly studies indicate that AMPK is also activated by cellular stresses in a non-canonical way where the level of AMP/ADP or Ca^{2+} is indifferent (Hardie et al., 2012).

Due to the tumor suppressive function of LKB1, AMPK appears to be a component in the tumor suppressor cascade mediated by LKB1 (Bon et al., 2015). Knocking out of the catalytic subunit of AMPK accelerates the development of lymphomas with ectopic c-Myc expression (Faubert et al., 2013). In addition, AMPK is a “metabolic” tumor-suppressor by repressing de novo lipognesis. Since de novo fatty acid is required for G2-M phase, APMK would arrest cell cycle at G2-M checkpoint (Scaglia et al., 2014). Interestingly, AMPK phosphorylates BRAF at Ser729, which prevents the interaction between BRAF and the scaffolding protein kinase suppressor of Ras 1 (KSR1). The oncogenic MEK-ERK pathway is suppressed subsequently and the cell prolieferation is also impaired (Shen et al., 2013).

I.5. TXNRD2 AND CANCER

The major antioxidant enzyme system mainly contains thioredoxin (TRX) and glutathione (GSH) systems that maintain homeostasis and redox balance. Impaired function of one of the systems results in a compensatory up-regulation of the other (Benhar et al., 2016; Jovanovic et al., 2022; Yan et al., 2019). Over-activated TRX system is commonly observed in different cancers, such as breast (Bhatia et al., 2016), cervical (Du et al., 2012), colorectal (Marmol et al., 2019) and pancreatic cancer (Arnold et al., 2004). The deregulation of TRX system in these cancers promotes progression and development as well as contributes to drug resistance (Arnold et al., 2004; Kim et al., 2005; Marmol et al., 2019). TRX system contains TRX, thioredoxin reductases (TXNRDs), thioredoxin-interacting proteins (TXNIPs) and nicotinamide adenine dinucleotide phosphate (NADPH) (Jovanovic et al., 2022). TRX1/TXNRD1 mainly presents in the cytoplasm whereas TRX2/TXNRD2 appears in the mitochondria. However, TRX and TXNRDs are released into peripheral blood from tumor cells, which is supposed to protect tumor cells from the challenge of extracellular oxidation (Soderberg et al., 2000).

The cytosolic selenoprotein thioredoxin reductase 1 (TXNRD1) is a central regulator of the Trx system and it is considered as a druggable target to achieve selective cancer cell killing (Anestal et al., 2008; Arner, 2017; Becker et al., 2000; Cebula et al., 2015; Fang et al., 2005; Stafford et al., 2018; Wang et al., 2012; B. Zhang et al., 2017). ROS is produced from many sources such as glycerol-3-phosphate dehydrogenase (GPDH), dihydroorotate dehydrogenase (DHODH) and monoamine oxidases (MAOs) (Purohit et al., 2019). The antioxidant capacity of mitochondria can also be determined by mitochondrial peroxiredoxin (PRX3) which is sustained by mitochondrial TRX2 and TXNRD2 (Cox et al., 2009; Rabilloud et al., 2001). Since the GSH and mitochondrial

TRX2 constitute the activity of PRX3 (Zhang et al., 2007), the crosstalk between the GSH system and the TRX system exists in regulation of mitochondrial redox status.

Unlike TXNRD1, targeting TXNRD2 is difficult due to the poor efficiency of drug delivery with the requirement of accumulation in mitochondria. Currently, many Txnrd inhibitors commonly target both TXNRD1 and TXNRD2. Previous studies identify that TXNRD1 inhibitors could induce cell death that is driven by the dysfunction of mitochondria, whereas it is still an obstacle to distinguish the inhibitory effect of those pan-inhibitors on TXNRD2 (Anestal et al., 2008; Cenas et al., 2004; Eriksson et al., 2009; Rigobello et al., 2005). In a recent study, Wogonin, a flavonoid derived from *Scutellaria baicalensis*, has been validated to repress TXNRD2 specifically in breast cancer. In this case, due to the repression of TXNRD2 mediated by Wogonin, ROS is accumulated in breast cancer cells, which increases the expression p16 and leads to cellular senescence (Yang et al., 2020).

I.6. The Aims of the Study

Our study aimed to elucidate the role of TXNRD2 in the progression of pancreatic cancer, especially the role of TXNRD2 in EMT and metastasis in pancreatic cancer.

II. Materials and Methods

II.1. Standard chemicals (Table II.1)

Chemicals	Article Number	Company
Ammonium persulfate(APS)	A3678	Sigma-Aldrich
Auranofin	A6733	Sigma-Aldrich
Bovine Serum Albumin (BSA)	A4503-100G	Sigma-Aldrich
Bromophenol Blue	B0126	Sigma-Aldrich
Complete Tablets Mini EASYpack	04693124001	Roth
cOmplete™, Mini Protease Inhibitor Cocktail	04693124001	Roth
Crystal Violet	C0775	Sigma-Aldrich
Dimethyl Sulfoxide (DMSO)	D8418	Sigma-Aldrich
DL-Dithiothreitol (DTT)	9163	Sigma-Aldrich
D-Mannitol	M4125-100G	Sigma-Aldrich
Doxycycline hyclate	D9891	Sigma-Aldrich
Dulbecco's Modified Eagle Medium	41965062	Thermo Fischer Scientific
Ethanol, absolute	1.00983.1000	Merck
Fetal Bovine Serum	10270106	Thermo Fischer Scientific
Glutaraldehyde	3778.1	Roth
Glycine	50046-1KG	Sigma-Aldrich
Hydrochloric acid (HCL)	7647-01-0	Roth
Isopropanol	109634	Merck
jetPRIME®	101000015	Polyplus

Methanol	CP43.4	Roth
Minimum Essential Medium Non-Essential Amino Acids	11140-035	Gibco™
Nonidet P 40 Substitute	74385-1L	Sigma-Aldrich
PBS Dulbecco	L182-50	Merck
PhosSTOP EASYpack	04906837001	Roth
Puromycin	P8833	Sigma-Aldrich
Skim Milk Powder	70166-500G	Sigma-Aldrich
Sodium Chloride (NaCl)	71376-5KG	Sigma-Aldrich
Sodium Deoxycholate	D6750-500G	Sigma-Aldrich
Sodium dodecyl sulfate (SDS)	2362.2	Roth
Sodium hydroxide solution (NaOH)	T198.1-1L	Roth
Sterile DPBS	14200075	Gibco™
Sucrose	S0389-500G	Sigma-Aldrich
Tris	5429.2	Roth
Tris-HCl	9090.3	Roth
Trypsin-EDTA (0.05%), phenol red	25300054	Gibco™

II.2. Buffers and Solutions (Table II.2)

Western blots	
Regeants	Recipes
6x SDS Sample buffer (10ml)	7 ml Stacking Buffer 3 ml Glycerin

	1 g SDS 1.2 mg Bromophenol Blue 0.93 g DTT add deionized water (diH2O) to 10 ml
RIPA Buffer (100 ml)	5 ml Tris-HCl (pH 7.5) 3 ml NaCl (5 M): 1 ml NP-40 0.5 g Sodium Deoxycholat 500 µl SDS (20%) fill up to 100 ml with deionized water (diH2O)
20% SDS (100 ml)	20 g SDS 100 ml deionized water (diH2O)
10% APS (10 ml)	1 g APS 10 ml deionized water (diH2O)
Stacking Buffer (pH 6.8, 100 ml)	6.05 g Tris-Base 0.4 g SDS adjust pH to 6.8 with 1 M HCl fill up to 100 ml with deionized water (diH2O)
Separation Buffer (pH 8.8, 500 ml)	30.3 g Tris-Base 0.67 g SDS adjust pH to 8.8 with 1 M HCl fill up to 100 ml with deionized water (diH2O)
10% SDS polyacrylamide gel (1.5 mm) Separation Gel	3.9 ml Rotiphorese® Gel 30 (37.5:1) 2.9 ml Separation Buffer (pH 8.8) 4.8 ml deionized water (diH2O)

	70 µl 10% APS 14 µl TEMED
10% SDS polyacrylamide gel (1.5 mm) Stacking Gel	0.6 ml Rotiphorese® Gel 30 (37.5:1) 1.2 ml Stacking Buffer (pH 6.8) 2.8 ml deionized water (diH2O) 46.7 µl 10% APS 9.3 µl TEMED
10x Tris Buffered Saline (10 x TBS, 1000 ml)	80 g NaCl 31.5 g Tris HCl adjust pH to 7.6 fill up to 1000 ml with deionized water (diH2O)
1xTris Buffered Saline with Tween-20 (1 x TBS-T, 1000 ml)	100 ml 10 x TBS 1 ml Tween-20 fill up to 1000 ml with deionized water (diH2O)
10x Tris Glycine SDS Running Buffer (1000 ml)	30.2 g Tris 144 g Glycin 50 ml 20% SDS fill up to 1000 ml with deionized water (diH2O)
10x Tris Glycine Transfer Buffer (1000 ml)	144 g Glycin 30 g Tris-Base fill up to 1000 ml with deionized water (diH2O)

1x Tris Glycine Transfer Buffer (1000ml)	100 ml 10 x Tris Glycine Transfer Buffer 200 ml Methanol 700 ml deionized water (diH2O)
1 x Blocking buffer: (milk)	5 g skim milk powder dissolved in 100 ml 1 X TBST
1 x Blocking buffer:(BSA)	5 g BSA dissolved in 100 ml 1 X TBST.
10 x Phosphatase inhibitor solution:	1 Tablet (PhosSTOP EASYpack) dissolved in 1 ml of deionized water
25 x Protease inhibitor solution	1 Tablet (Complete Tablets Mini EASYpack) dissolved in 2 ml of deionized water
Colony formation	
Fixation solution (100 ml)	24 ml Glutaraldehyde 0.5 g (w/v) Crystal Violet 76 ml deionized water. Stored at room temperature.

II.3. STANDARD DEVICES (TABLE II.3)

Product	**Supplying company**

Axiovert 200M	Zeiss
Axiovert 40 CFL	Zeiss
Centrifuge 5147 R	Eppendorf
Centrifuge 5702 R	Eppendorf
Countess II Automated Cell Counters	Thermo Fisher Scientific
Eppendorf Pipette Set Research Plus	Eppendorf
FLUOstar Omega microplate reader	BMGs Labtech
FLUOstar OPTIMA microplate reader	BMGs Labtech
Gel DocTM XR system	Bio-Rad
HeracellTM 240 incubator	Thermo Fisher Scientific
Herasafe class II biological safety cabinet	Thermo Fisher Scientific
LightCycler 480	Roth Diagnostics
Mini-PROTEAN Tetra Vertical Electrophoresis Cell	Bio-Rad
Mini Trans-Blot Electrophoretic Transfer Cell	Bio-Rad
NanoDrop 2000	Thermo Fisher Scientific
Pipette Controllers	Falcon™
PowerPac™ Basic	Bio-Rad
ThermoMixer compact	Eppendorf

II.4. CELL CULTURE

Cells used in the experiments were maintained in complete DMEM medium (The basic DMEM medium containing 10% FBS, 1% Penicillin-Streptomycin and 1% Minimum Essential Medium Non-Essential Amino Acids) in 20% O_2 and 5% CO_2 and 37 °C. Auranofin was dissolved in DMSO at 10 mM and used at the final concentration of 1

μM. Doxycycline (DOX) was dissolved in DMSO at 1 mM and used at the final concentration of 1 μM.

II.5. CRISPR/CAS9 TECHNOLOGY

To generate *Txnrd2*-deficient tumor cell lines, a double nicking approach of the CRISPR/Cas9 technology was used in the project. Two designed sgRNAs targeting *Txnrd2* (Txnrd2_A and Txnrd2_B) were inserted into pX462 plasmid (performed by Kerstin Pfister). Next, plasmid containing sgRNAs were transfected into tumor cells by using jetPRIME DNA and siRNA transfection reagent according to the instructions provided by the manufacturer. After 24 hours of transfection, fresh selection medium (1.5 μg/ml puromycin in the culture medium) was added to replace the old medium. Cells were kept in cell culture medium with puromycin after selection. Western blot analysis was performed to validate the deletion of *Txnrd2* in tumor cells. The sequences of sgRNAs is listed in Table II.4

Table II.4 Sequences used for sgRNA

Oligos	(5’ -> 3’)
Txnrd2_cc_A_FWD	CACCGAAGCCATGACTCCTAGACGA
Txnrd2_cc_A_REV	TCGTCTAGGAGTCATGGCTTC
Txnrd2_cc_B_FWD	CACCGTGTCTGGATTGCCTACCTCG
Txnrd2_cc_B_REV	CGAGGTAGGCAATCCAGACAC

II.6. TOTAL RNA ISOLATION

After different treatments, the total RNA of cells was collected and isolated by using Maxwell® 16 LEV simplyRNA Purification Kits (Promega) and the Maxwell® 16 Instrument (Promega). The concentration and quality of the RNA were analyzed by using a NanoDrop 2000 (Thermo Fisher Scientific). RNA samples were stored at -80 °C before used in following experiments .

II.7. Protein isolation

After the cell confluency reached 70% in a 10 cm cell culture dish, cells were washed twice with PBS. Next, added cold 400 µl of RIPA lysis buffer containing 40 µl of 1X Phosphatase Inhibitor Solution and 10 µl of 1X Protease Inhibitor into the dishes and keep it incubating on ice for 10 min.Then cell lysate was collected into a fresh tube and centrifuge at 10,000 g at 4 °C. The supernatant was transferred into a new tube and stored at -80 °C before use. The concentration of protein was determined by using the Pierce™ BCA Protein Assay Kit according the instruction provided by the manufacturer. Protein lysis and isolation were performed on ice.

II.8. Mitochondria isolation

A Mitochondria Isolation Kit (MITOISO2 kit,Sigma) was utilized to isolate mitochondria. Briefly, cells were seeded into a 20 cm dish before the experiments. After the cell's confluency reached around 90%, cell samples were trypsinized and collected. Cells were then pelleted for 5 min at 600 g. The cell pellet was resuspended in cold PBS and centrifuged again for 5 min at 600 g at 4 °C, this was repeated twice, supernatants

were discarded. Cell pellets were resuspended in 1X Extraction Buffer A (1 ml/ 2 x10^7 cells), the suspension was incubated on ice for 15 min. Next, a dounce 15 ml homogenizer was used for 30 strokes to homogenate the cells on ice. The homogenate was centrifuged at 600 x g for 10 min at 4 °C. The supernatant was transferred to a new 1.5 ml tube and then centrifuged at 11,000 g for 10 min at 4 °C. After this, the supernatants were discarded and the pellets were resuspended in 200 µl of CelLytic M Lysis Reagent with Protease Inhibitor Cocktail (1:100 [v/v]) to perform the Txnrd activity assay.

II.9. THIOREDOXIN REDUCTASE ACTIVITY ASSAY

The samples for measurement were obtained from the mitochondria isolation. Samples and buffers were added to a 96-well plate according the Table II.5 below. The DTNB solution was added just before the start of the measurement. A FLUOstar OPTIMA microplate reader (BMG Labtech) was used to measure the absorption at a wavelength of 412 nm for 2 min in intervals of 10 seconds. The activity of thioredoxin reductase activity was calculated as follows: Activity (units/protein = sample slope*0.2/0.01/0.55/sample protein concentration.

Table II.5 Reaction Scheme for a 96-Well Plate (200 µl) Assay.

Sample type	Enzyme (µl)	1xAssay Buffer (µl)	Diluted Inhibitor Solution (µl)	Working Buffer (µl)	DTNB (µl)
Blank	0	14	0	180	6
Positive	2	12	0	180	6
Sample	10	4	0	180	6

Sample+ inhibitor	6	4	4	180	6

II.10. PROLIFERATION ASSAYS

Cell proliferation rate was determined by using a CyQuant Assay Kit (C7026, Thermo Fisher Scientific) according to the instructions provided by the manufacturer. Briefly, cells were seeded into a bottom-clear black 96 well plate at a density of 1000 cells / well in triplicates. Replicate microplates were prepared for measurement at different time points (0 h, 24 h, 48 h and 72 h). 200 µl media was added to each well. At the desired time point, medium was was removed by aspiration using vacuum pump and then by blotting the plate on the paper towels. The microplates were stored at -80 °C before the analysis. For quantification of samples, microplates were thawed at room temperature. Next, 200 µL of CyQUANT® GR dye/cell-lysis buffer was added to each sample well and gently mixed. The mixture was incubated at room temperature for 2-5 min protected from the light. A FLUOstar OPTIMA microplate reader (BMG Labtech) was used to measure the fluorescence of samples at the wavelength of 480 nm (excitation) and 520 nm (emission). The fluorescence values of different timepoints were normalized to the value of 0 h. The results were presented with mean values of replicates.

II.11. COLONY FORMATION ASSAY

Cells were seeded into a 6-well plate at a density of 500 cells/well and the wells were filled with 2 mL fresh medium. During incubation (7 days), 1 mL of medium was removed and replaced with fresh medium every two days. After 7 days, cells were fixed and stained by prepared fixation solution (1 ml/well) for 30 min following the wash step with PBS until the crystal violet in solution was totally removed. Pictures of plates were taken by a scanner (EPSON PERFECTION V600 PHOTO) and imported into the Fiji Software for colony area analysis.

II.12. ROS ASSAY

CellROX Green Reagent (C10444, Invitrogen) was used to determine ROS levels according to the instructions provided by the manufacturer. Briefly, cells were seeded into a bottom-clear black 96-well plate (Costar 3603, Corning Incorporated) at a density of 10,000 cells/well and filled with 200 µl medium. After 24-hours of incubation, CellROX Green Reagent was added into each well at a final concentration of 5 µM and mixed well and incubated for 30 mins at 37 °C. After incubation, medium was removed and cells were washed by PBS for 3 times. A FLUOstar Omega microplate reader (BMG Labtech) was used to measure the fluorescence of samples at the wavelength of 480 nm (excitation) and 520 nm (emission). The results were calculated and presented as relative ROS levels, which was determined by normalization of ROS fluorescence to the fluorescence indicating cell number as determined by CyQuant Assay Kit (C7026, Thermo Fisher Scientific).

II.13. QUANTITATIVE REAL-TIME PCR (RT-PCR)

Before qRT-PCR, total RNA was reverse transcribed to cDNA by using the SuperScript II Enzyme. The reaction mix contained 0.5 µL of Random Primers (C118A, Promega), 1 µl of 10 mM dNTP Mix (18427-013, invitrogen™) and 1 µl of RNA. The reaction mix was incubated at 65 °C for 5 min and put on ice. Next, 4 µL of First Strand Buffer (of SuperScript II Reverse Transcripase system; 18064-014, invitrogen™) and 2 µl M DTT (Y00147, invitrogen™) were added into the reaction mix. The reaction mix at 25 °C for 2 min. Finally, 1 µl of SuperScript II Enzyme was added and the reaction mix was incubated for 10 min at 25 °C, 50 min at 42 °C and 15 min at 70 ℃. The reaction was performed in a Mastercycler, Eppendorf.

The synthesized cDNA was diluted with PCR-grade water at a ratio of 1:20. 4 µl of diluted cDNA were used for qRT-PCR reaction together with 10 µl of LightCycler 480 SYBR Green (10559520, Roth), 1 µl of Primer Mix (for example,Txnrd2) and 5 µl of PCR-grade water in each reaction. The reaction was performed in a Roth LightCycler 480 platform with the following program: initial denaturation (95 °C, 10 min), 40 cycles of denaturation (95 °C, 20 sec), annealing (52 °C, 30 sec), and elongation (72 °C, 25 sec) with single acquisition, followed by a melting curve analysis consisting of a 65 to 97 °C temperature gradient at a ramp rate of 0.11 °C/second with acquisition every 5 °C. The specificity of the PCR reaction was verified by the obtained melting curve after the PCR reaction. Gene expression was normalized to *Cyclophilin* by using the ΔΔCt method described in (Livak & Schmittgen, 2001). The primers used for RT-PCR are listed in Table II.6.

Table II.6 Primers used in RT-PCR analysis.

Target genes	Primer sequences (5’-3’)

Cdh1	Forward: ATGAGCGTGCCCCAGTATCGTC Reverse: CAGGCTAGCGGCTTCAGAACCA
Cyclophilin	Forward: ATGGTCAACCCCACCGTG Reverse: TTCTGCTGTCTTTGGAACTTTGTC
Twist	Forward: TCCAGAGAAGGAGAAAATGG Reverse: GGTCTCTGCTCTTCTAATTTCC
Txnrd2	Forward: CAGGTCACTAGGCTGTAGAGTTTGC Reverse: ATGTCCCAGTGTACTTATGATGAATC
Vim	Forward: CCTGTACGAGGAGGAGATGC Reverse: GTGCCAGAGAAGCATTGTCA

II.14. WESTERN BLOT ANALYSIS

Western blot analysis was performed after protein isolation. The concentration of protein was determined by BCA assay with the Pierce™ BCA Assay Kit (Thermo Fisher Scientific; 23225). Samples were prepared by mixing the lysate and 6XSDS sample buffer (5:1). The protein samples were heated to 95 ℃ for 5 min in a Thermomixer® compact (Eppendorf) and stored at -20 °C. Protein were loaded onto 10% SDS-polyacrylamide gel for electrophorese (SDS-PAGE) in an Electrophoresis Chamber (Mini-PROTEAN Tetra Vertical Electrophoresis Cell, Bio-Rad) with a power supply (PowerPac™ Basic, Bio-Rad). The Spectra™ Multicolor Broad Range Protein Ladder (26634, Themo Fisher Scientific) served as a molecular weight marker. Before protein samples reached the separating gels, the voltage was kept at 80 V, and then the voltage was increased to 200 V until the protein samples reach the end of SDS-PAGE gel. Next, protein was transferred on to a Amersham Protran Premium 0.2 NC

nitrocellulose Western blotting membrane (cytiva,10600011) or Amersham Protran Premium 0.45 NC nitrocellulose Western blotting membrane (cytiva,10600012) at 100 V for 120 min in Electrophoresis Chamber with Mini Trans-Blot® Module (Mini Trans-Blot Electrophoretic Transfer Cell, Bio-Rad). Then the membrane was blocked using 5% skim milk or 5% BSA dissolved in TBST for 1 h at room temperature. Next, the membrane was incubated with the primary antibody diluted in the blocking solution according to the instruction from the manufacturer at 4 °C overnight. After that, the membrane was washed 3 times (10 min each time) with 1XTBST and incubated with the secondary antibody diluted in the blocking solution (1:5000) for 1 hour at room temperature. After washing 3 times with TBST, the membrane was used for imaging by using the ECL reagent (RPN2106, GE Healthcare) and the ChemiDoc™ XRS+ (Bio-Rad). Western Blot bands were analyzed with Fiji Software as described before (Gallo-Oller et al., 2018). Antibodies used in Western blot analysis are listed in the Table II.7.

Table II.7 Antibodies used in western blot analysis.

Target protein	Brand/Company	Cat.number	Target Size
AMPK	Cell Signaling Technology	2532s	62 kDa
CATALASE	Cell Signaling Technology	14097	60 kDa
E-CADHERIN	BD Biosciences	610181	120 kDa
GPX8	proteintech	16846-1-AP	24 kDa
GSTT2	abcam	ab176336	28 kDa
HSP90	Cell Signaling Technology	4874	90 kDa
N-CADHERIN	Cell Signaling Technology	131161	140 kDa
p-AMPK	Cell Signaling Technology	2535s	62 kDa

PRDX1	Cell Signaling Technology	8499	21 kDa
PRDX2	Cell Signaling Technology	46855	23 kDa
SLUG	Cell Signaling Technology	9585	30 kDa
SOD2	Cell Signaling Technology	13141	22 kDa
TXNRD2	abcam	ab180493	57 kDa
VIMENTIN	Cell Signaling Technology	5741	57 kDa

II.15. PLASMID ISOLATION

Plasmids were transformed into KCM competent *E.coli* (Chung & Miller, 1988; Walhout et al., 2000). Briefly, 1-5 µl of DNA (up to 100 ng) were mixed with 40 µl of competent *E.coli* in a 1.5 ml EP-tube. The mixture was incubated on ice for 30 min. A Heat shock 42 °C was performed for 90 seconds, after which the mixture was put back on ice for 2-3 min. Added 900 µl of ampicillin-free LB medium into the mixture and grow at 37 °C for 1 h by gently shaking. Plated 50-100 µl transformed *E.coli* onto a 10-cm LB-agar plate containing ampicillin (100 µg/ml). Plates were incubated at 37 °C overnight. Grown clones were picked with pipette tips and were incubated in LB medium containing ampicillin (100 µg/ml) at 37 °C overnight.

The plasmid was isolated by using the PureYield™ Plasmid Miniprep System (Promega) according to the instruction provided by the manufacturer. Briefly, added 100 µl of Cell Lysis Buffer (Blue) to 600 µl of bacterial culture in a 1.5 ml tube. Inverted the mixuture 6 times. Added 350 µl of cold Neutralization Solution and mixed thoroughly by inverting. Centrifuged at maximum speed (10,000 g) for 3 minutes. Transferred the supernatant (900 µl) to a PureYield™ Minicolumn without disturbing the cell debris pellet. Placed the minicolumn into a collection Tube, and centrifuged at

maximum speed in a microcentrifuge for 15 seconds. Discarded the flowthrough, and placed the minicolumn into the same Collection Tube. Washed column with 200 µl of Endotoxin Removal Wash (ERB) for 15 seconds. 400 µl of Column Wash Solution (CWC) was used to wash the minicolumn membrane and discarded by Centrifuge at maximum speed for 30 seconds. Transfer the minicolumn to a clean 1.5 ml microcentrifuge tube, 30 µl of Elution Buffer or nuclease-free water was used to elute plasmid. Cap the microcentrifuge tube, store plasmid DNA at –20°C.

II.16. Restriction digestion of plasmid DNA

The restriction digestion was performed by employing restrictions endonucleases from NEB (New England Biolabs). Restriction mix was made in accordance with the manufacturer's guidelines, incubated for a sufficient amount of time (either 4 or 16 hours), and at an appropriate temperature. Restriction digested plasmid DNA was separated on a 1% low melting point agarose gel at 80 to 100 V while being stained with ethidium bromide. The desired-sized fragment was cut with a scalpel. DNA was extracted from the gel piece using the Qiagen Gel Extraction Kit according to the instructions of the manufacturer (Qiagen).

II.17. Ligation of plasmid DNA

In accordance with the instructions in the manual, T4 DNA Ligase was utilized to ligate the necessary insert with the suitable plasmid backbone (New England Biolabs). The ultimate volume of a typical ligation mixture is 20 µl. Overnight, the ligation was done

at 16°C. Then, competent bacteria were transformed using the ligation mixture. After transformation, the required insert's successful integration into the vector was observed. Therefore, restriction digestion using carefully chosen endonucleases was applied to plasmid DNA from overnight cultures of single colonies. Using the SnapGene software, the restriction pattern following electrophoretic separation was compared to the plasmid map.

II.18. Cloning of Txnrd2 into the pINDUCER20 system

The expression vector pINDUCER20-*Txnrd2* was generated to study the function of Txnrd2 expression in pancreatic cancer cells. With *EcoRI* and *XhoI*, the P442 *Txnrd2* expression vector (received from AG Conrad) was digested to isolate the Txnrd2 fragment. After pENTR1A was digested with *EcoRI* and *XhoI*, the Txnrd2 fragment was inserted into the plasmid's backbone to create the entry clone pENTR1A Txnrd2 by ligation (Figure II.1).

For ligation, added the ingredients into reaction system according to Table II.8 in a 1.5 ml microcentrifuge tubes at room temperature. Incubated the system at 25°C for 1 hour to generate the expression vector. Next, 2 µl of Proteinase K was subsequently added into the system and incubated for 10 minutes at 37 °C.

Table II.8 Components of ligation system

Component	**Sample**
Entry clone (100-300 ng/reaction)	1-10 µl
pINDUCER20 (300 ng/reaction)	2 µl

5X LR Clonase™ Reaction Buffer	4 µl
TE Buffer, pH 8.0	to 16 µl

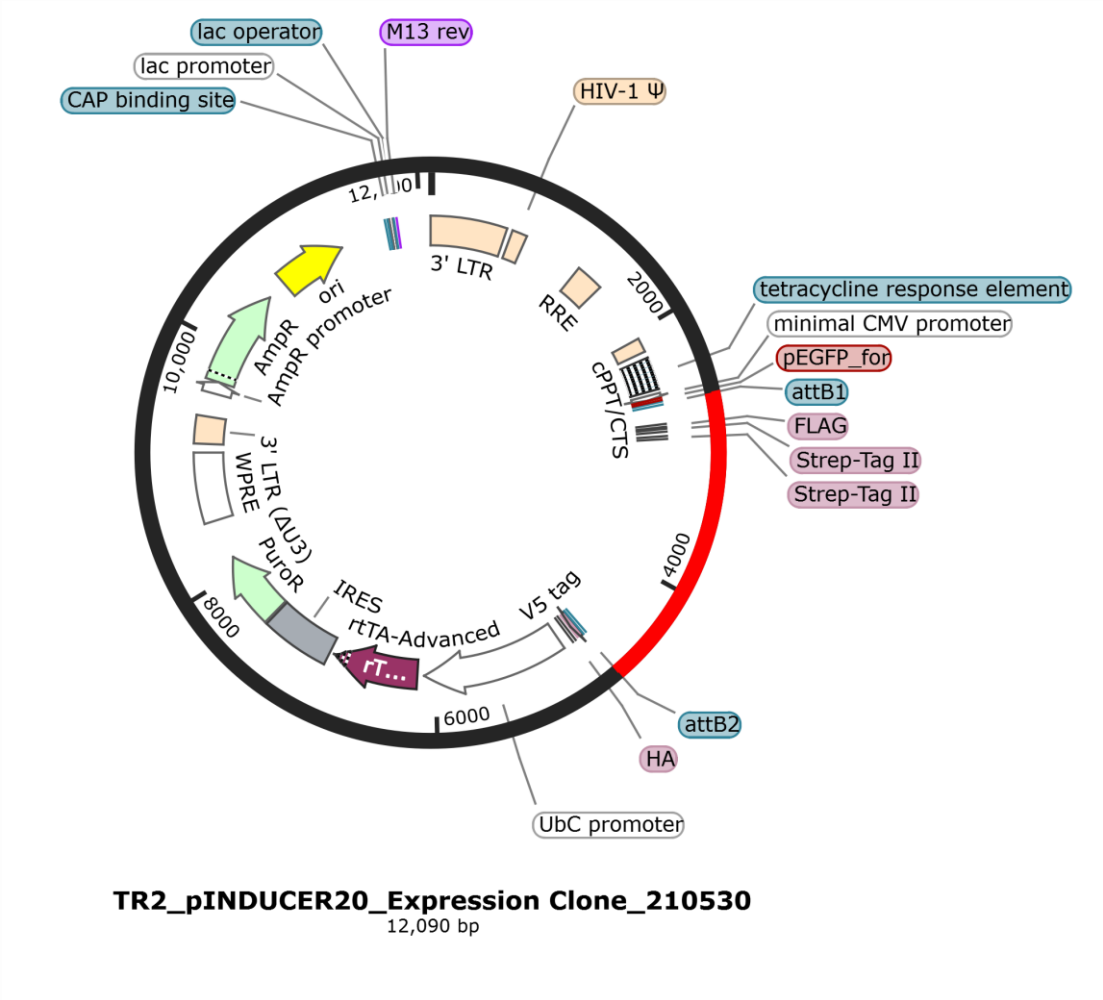

Figure II.1 The generated pINDUCER20_Txnrd2 map.

II.19. LENTIVIRUS PRODUCTION AND TRANSDUCTION

Seeded 1.5 x 10^6 293T packaging cells per 10 cm plate in complete DMEM. Incubated the cells at 37 °C, 5% CO_2 for 20 hours. Gently aspirated media, added 6 ml of fresh complete DMEM and incubated for 3 to 5 hours.

Before transfection, prepared a mixture of the 3 transfection plasmids (the amount of plasmids required showed in Table II.9).

Table II.9 The ratio of plasmids amount.

plasmids	ratios
psPAX	2
pECO 2	2
Txnrd2_pINDUCER20	3

Replaced the medium with 6 ml of P/S-free DMEM medium (containing 30% FCS) before transfection. The transfection was performed with jetPRIME reagent according to the instructions provided by the manufacturer. After 72 hours of transfection, the supernatant was collected and filtered through a 0.45 μm PES filter.

Lentivirus transduction was carried out in 6-well plates by incubating cells with virus according to Table II.10.

Table II.10 Transduction system.

Components	Total volume: 1 ml/well
Lentivirus (μl)	640
Polybrene 1 mg/ml (μl)	5
Medium (μl)	355

II.20. STATISTICAL ANALYSIS

Statistical analyses were performed with the GraphPad Prism Software, Version 7. Routinely, a two-sided student's t-test was used with each value representing the mean of experiments. A p-value of less than 0.05 was considered significant.

III. RESULTS

III.1. TXNRD2 IS ACTIVATED IN MESENCHYMAL CELL LINES DERIVED FROM CK MOUSE

To investigate the EMT in pancreatic cancer, primary cell lines were isolated from *Kras*$^{+/G12D}$ CK mice (cell lines received from AG Saur or generated in the AG Schmid/Einwächter). The derived cancer cells were categorized into two groups, namely *Kras*$^{+/G12D}$_epithelial (CK-EPI) and *Kras*$^{+/G12D}$_mesenchymal (CK-MES) according to their morphology. CK-EPI cells showed high frequency of typical epithelial morphology, whereas the shape of CK-MES cells was more spindle-like (Figure III.1A). Indeed, the expression of *Cdh1* was elevated in CK-EPI cells compared to CK-MES cells evaluated by RT-PCR. Conversely, both *Vim* and *Twist* were repressed in CK-EPI cells compared to CK-MES cells (Figure III.1B). Above results indicated that EMT is enhanced in CK-MES cells. Previous studies have shown that EMT is closely associated with ROS activity (Chatterjee & Chatterjee, 2020). Here, we confirmed a significant lower ROS level in CK-MES cells compared to CK-EPI cells (Figure III.1C). In addition , the expression of several antioxidant proteins was tested by western blot analysis. Many components of antioxidant systems including TXNRD2, PRDX1, PRDX2, GSTT2, GPX8 and SOD2 were increased in most CK-MES cell lines (Figure III.1D). Of note, only the protein expression of TXNRD2 was higher in CK-MES cell lines, while mRNA levels were comparable (Figure III.1E and III.1F). TXNRD2 is a type of reductase critical for maintaining the function of thioredoxin-2 that converts NADPH to $NADP^+$ (Bradshaw, 2019). Therefore, the function of TXNRD2 may mainly rely on its enzymatic activity. Then, the enzymatic activity of TXNRD2 was analyzed and the result showed that the TXNRD2 activity was higher in CK-MES cells relative

to CK-EPI cells (Figure III.1G). Taken together, TXNRD2 is positively correlated with EMT in pancreatic cancer cell lines.

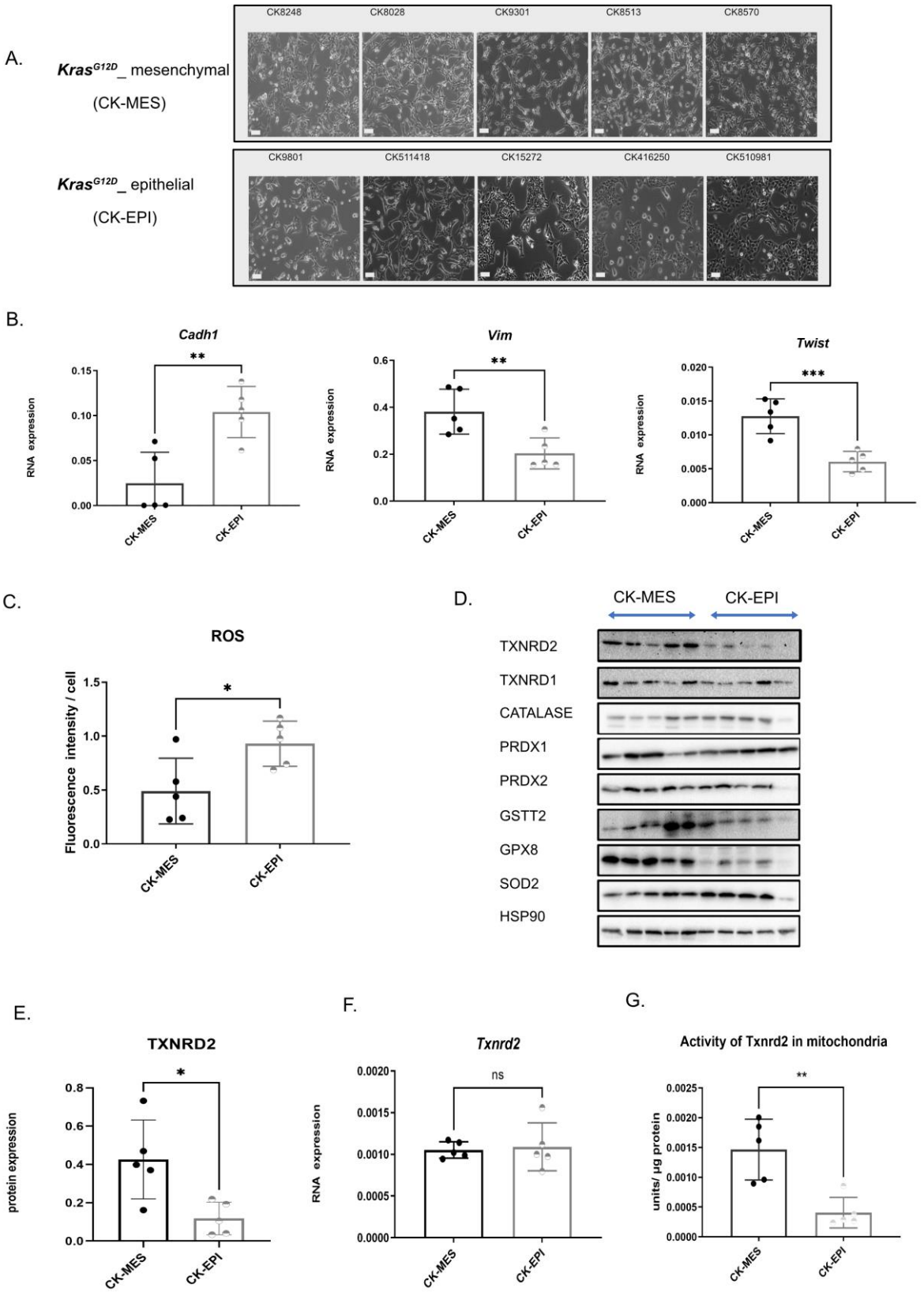

Figure III.1 Morphology of CK-MES/EPI tumor cell lines and expression of EMT marker and Txnrd2.

(A) 5 tumor cell lines with mesenchymal morphology and 5 tumor cell lines with epithelial morphology were isolated from CK mice. Microscope images were taken at 10x magnification. Scale bar, 100 µm

(B) The expression of *Cdh1*, *Vim*, *Twist* mRNA levels was quantified by RT-PCR in CK-MES (n = 5) and CK-EPI (n = 5) cells. Data are expressed using mean ± SD. Statistical results shown here by ** ($p < 0.01$), *** ($p < 0.001$).

(C) The ROS levels of CK-MES (n = 5) and CK-EPI cells (n = 5) were determined by CellROX Green. The results were normalized to cell number and were expressed using mean ± SD. Statistical results shown here by * ($p < 0.05$).

(D) Several antioxidant proteins were analyzed by using Western blotting in CK-MES (n = 5) and CK-EPI (n = 5) cells. HSP90 served as a loading control.

(E) TXNRD2 protein level and (F) *Txnrd2* mRNA level were measured by western blotting and RT-PCR respectively. Data are expressed using mean ± SD. Statistical results are represented by ns (not significant, $p \geq 0.05$), *($p < 0.05$).

(G) Enzymatic activity of TXNRD2 was validated by thioredoxin reductase assay. Data are expressed using mean ± SD. Statistical results shown here by ** ($p < 0.01$).

III.2. Repression of TXNRD2 inhibits EMT in pancreatic cancer cell lines

Since TXNRD2 showed a higher expression and enzymic activity in CK-MES cells compared to CK-EPI cells, here we wanted to know whether TXNRD2 is associated with EMT in pancreatic cancer. To this end, we performed RNA-seq analysis on both CK-MES and CK-EPI cells. Before sequencing, five CK-MES cells and five CK-EPI cells were treated with Auranofin (1 μM) or control medium for 1 week in 6-well plates. RNA was isolated subsequently and sequenced by Dr. Rupert Öllinger. RNA-seq results showed that both CK-MES and CK-EPI had decreased EMT signature in response to Auranofin, but only the decrease in CK-MES cells was significant (Figure III.2A). In Western blot analysis, Auranofin increased the expression of E-CADHERIN and β-CATENIN, whereas VIMENTIN and SLUG were repressed by Auranofin in CK-MES cells. Notably, Auranofin only showed slight impact on the protein level of N-cadherin in CK-MES cells (Figure III.2B). Furthermore, Auranofin treatment increased the level of ROS in CK-MES cells compared to untreated CK-MES cells (Figure III.2C), indicating that ROS is induced following TXNRD2 repression. Taken together, repression of TXNRD2 results in an inhibition of EMT and elevated ROS level in pancreatic cancer cells.

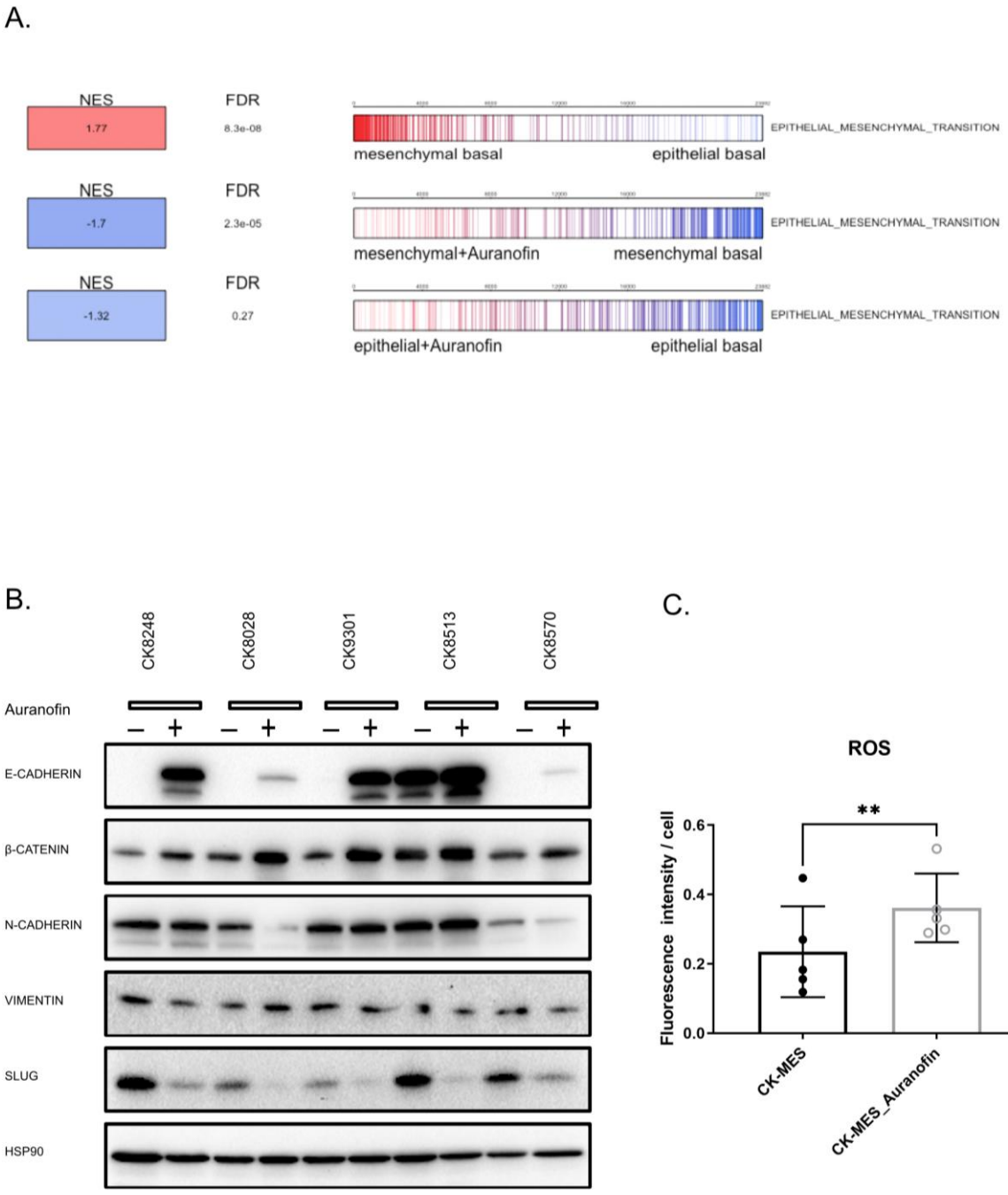

Figure III.2: Inhibition of Txnrd2 by Auranofin promotes MET.

(A) Gene set enrichment analysis for the Hallmark geneset EMT in CK-MES and CK-EPI cells after treated by Auranofin (1 μM) for 1 week. *NES* normalized enrichment score; *FDR* false discovery rate.

(B) CK-MES cell lines were treated with Auranofin (1 μM) for 1 week. Protein expression of E-CADHERIN, VIMENTIN, β-catenin and N-CADHERIN was checked by Western blotting in CK-MES (n = 5) cells after treated with Auranofin (1 μM) for 1 week. HSP90 served as a loading control.

(C) The ROS level was determined in CK-MES (n = 5) by CellROX Green after treated with Auranofin (1 μM) for 1 week. The results were normalized to cell number and are expressed using mean ± SD. Statistical results shown here by ** ($p < 0.01$).

III.3. Repression of TXNRD2 by Auranofin inhibited progression of pancreatic cancer

To demonstrate the function of TXNRD2 in pancreatic cancer, the proliferation and migration of pancreataic cancer cells were evaluated by colony formation assay and scratch assay respectively. The proliferation of CK-MES and CK-EPI cells was repressed to 85% and 80%, respectively, after Auranofin treatment. The proliferation ability of CK-MES was still higher than CK-EPI cells even in the presence of Auranofin (Figure III.3A and III.3B). In addition, the colony formation capability of CK-MES and CK-EPI cells was reduced by Auranofin (Figure III.3C and III.3D). Furthermore, Auranofin largely supressed migration ability of CK-MES and CK-EPI cells by 27.5% and 24.3% respectively (Figure III.3E and III.3F). Taken together, the TXNRD2 inhibitor Auranofin significantly inhibited proliferation and migration of pancreatic cancer cells.

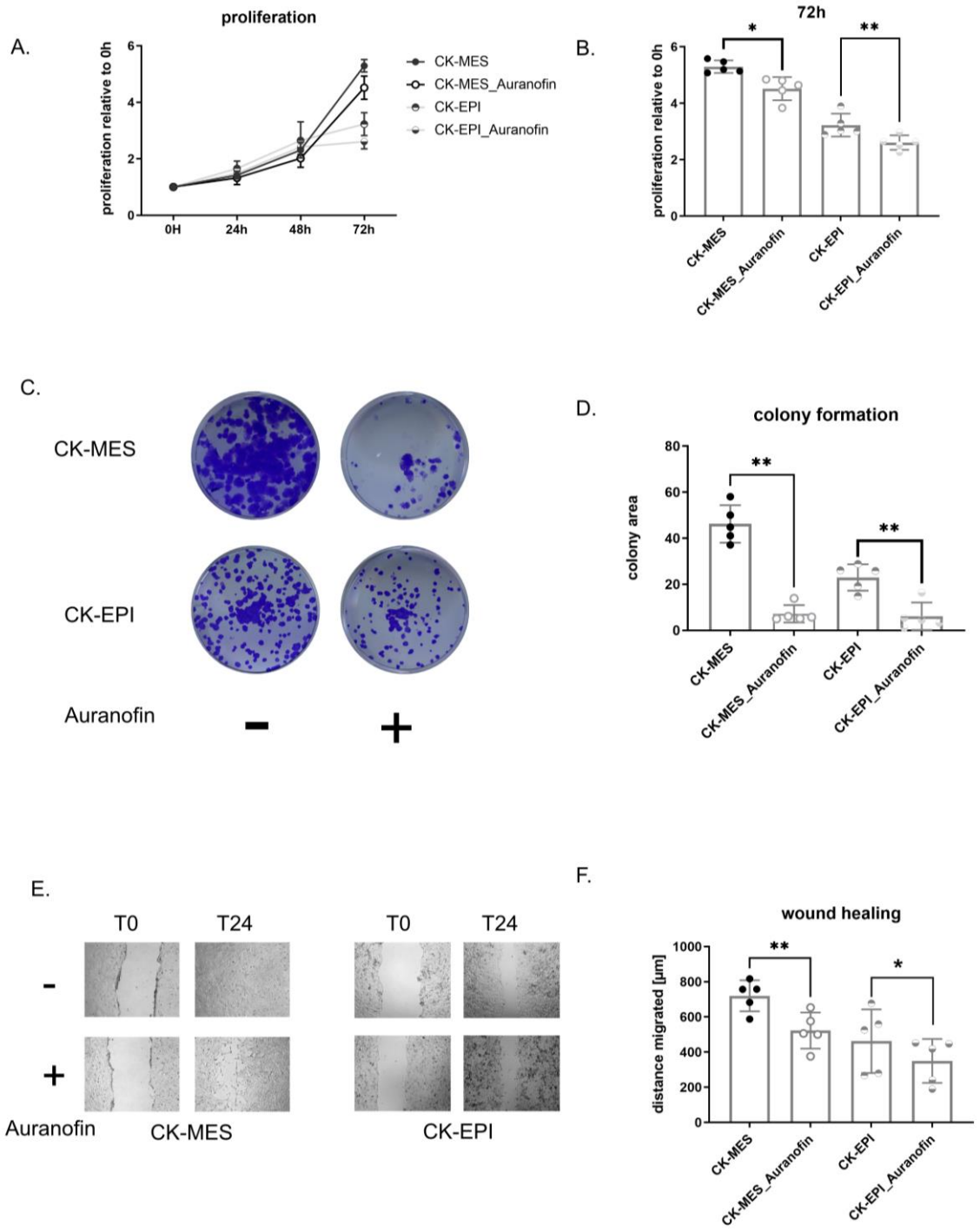

Figure III.3: Impaired proliferation, colony formation, and migration ability in the presence of Auranofin

(A) The proliferation of CK-MES and CK-EPI cell lines was evaluated by CyQuant Assay after treated cells with Auranofin (1µM) for the indicated periods. The results of each time point were normalized to the result of time point 0 h.

(B) The proliferation of CK-MES (n = 5) and CK-EPI (n = 5) cell lines was evaluated by CyQuant Assay after treated cells with Auranofin (1μM) for 72 h. The result of 72 h was normalized to the result of 0 h. Data are expressed using mean ± SD. Statistical results shown here by *($p < 0.05$), ** ($p < 0.01$).

(C) The colony forming capacity of CK-MES and CK-EPI cells was evaluated by colony formation assay after cells had been treated with Auranofin (1 μM) for 1 week. The representative pictures of colony formation assay are shown in (C). Quantification of colony formation assay was presented in (D). Data are expressed using mean ± SD. Statistical results shown here by ** ($p < 0.01$).

(E) The migration ability of CK-MES and CK-EPI cells was evaluated by a scratch assay after cells treated with Auranofin (1 μM) for 24h. Representative pictures of scratch assay are shown in (E). Quantification of colony formation assay was presented in (F). Data are expressed using mean ± SD. Statistical results shown here by *($p < 0.05$), ** ($p < 0.01$).

III.4. Inhibition of TXNRD2 results in AMPK activation

Previous studies have shown that AMPK functions as a sensor for metabolic stress and mediates redox balance. In addition, the activated AMPK leads to the inhibition of mTOR, thereby decreasing protein synthesis and increasing autophagy (Rabinovitch et al., 2017). Here, we would like to know whether the inhibition of TXNRD2 by Auranofin impacts AMPK activation. Indeed, CK-MES cells treated with Auranofin showed higher levels of phosphorylated AMPK, indicating that AMPK was activated by Auranofin (Figure III.4A). However, the expression of total AMPK protein was comparable with or without Auranofin treatments in CK-MES cells (Figure III.4B).

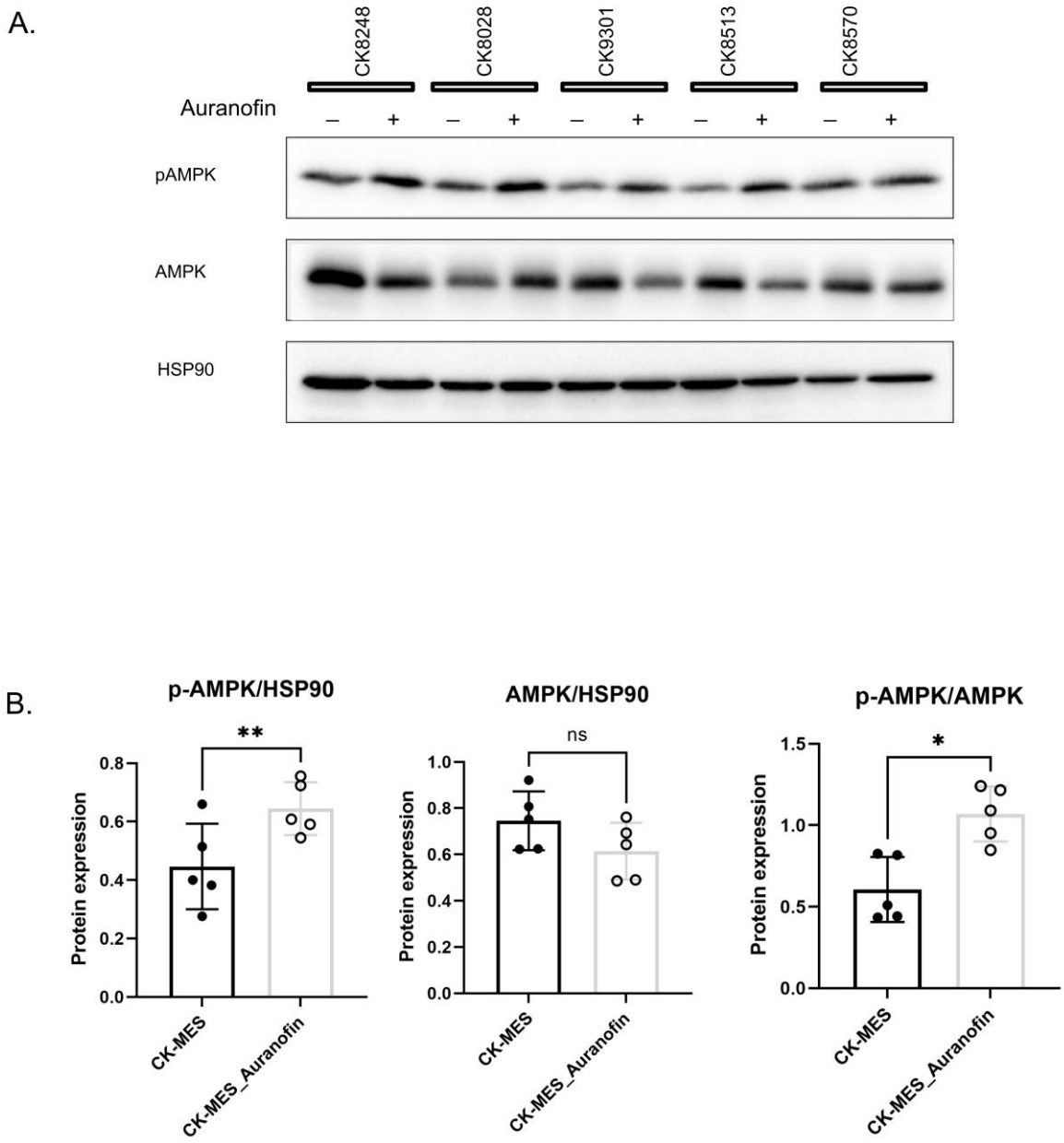

Figure III.4: TXNRD2 inhibition results in AMPK activation.

(A) The protein level of pAMPK and AMPK was determined by Western blotting in 5 CK-MES cancer cell lines after treated with Auranofin (1 μM) for 1 week. HSP90 sereved as a loading control.

(B) Quantification of pAMPK, AMPK and the ratio of pAMPK/AMPK protein expression in CK-MES with/without Auranofin treatment in (A). The protein expression was

normalized to Hsp90 and then compared with Auranofin untreated group (n = 5). Data are expressed using mean ± SD. Statistical results shown here by ns (not significant, $p \geq 0.05$), *($p < 0.05$), ** ($p < 0.01$).

III.5. *Txnrd2*-deficient pool generation and EMT markers evaluation

Since it had been identified that chemical inhibition of TXNRD2 inhibits the proliferation and migration of pancreatic cancer cells, next we aimed to uncover the function of TXNRD2 in pancreatic cancer cells by using CRISPR/Cas9 technology to abrogate the expression of *Txnrd2* in CK-MES cells and *Txnrd2* knockout was validated by Western blot (Figure III.5A). The generated clones were desginated with CK-MES_KO. The enzymatic activity of TXNRD2 was largely repressed in these CK-MES_KO cells compared to CK-MES cells (Figure III.5B). In line with the Auranofin results, E-CADHERIN and β-CATENIN were increased in *Txnrd2*-deficient CK-MES cells, whereas the expression of N-CADHERIN and SLUG was repressed in *Txnrd2*-deficient CK-MES cells (Figure III.5C). This results suggest that deletion of *Txnrd2* represses EMT markers in CK-MES cells. In addition, AMPK was activated in CK-MES_KO cells compared to *Txnrd2*-proficient CK-MES cells (Figure III.5C). ROS levels were also significantly higher in *Txnrd2*-deficient CK-MES cells compared to *Txnrd2*-proficient CK-MES cells (Figure III.5D). The observed results are comparable with the results of pharmacological inhibition by Auranofin.

A.

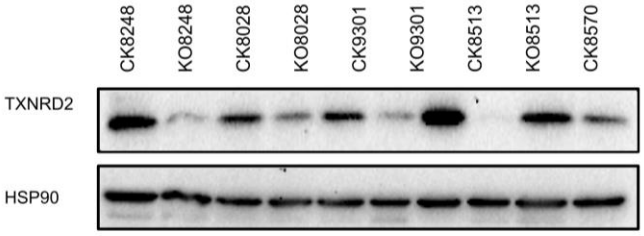
CK8248
KO8248
CK8028
KO8028
CK9301
KO9301
CK8513
KO8513
CK8570
TXNRD2
HSP90

B.

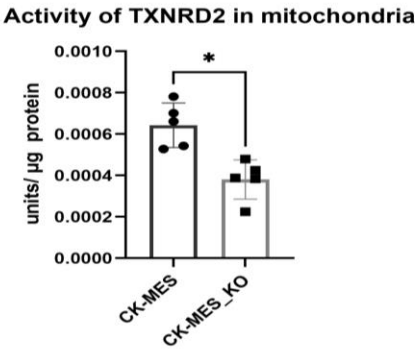
Activity of TXNRD2 in mitochondria
units/ µg protein
0.0010
0.0008
0.0006
0.0004
0.0002
0.0000
*
CK-MES
CK-MES_KO

C.

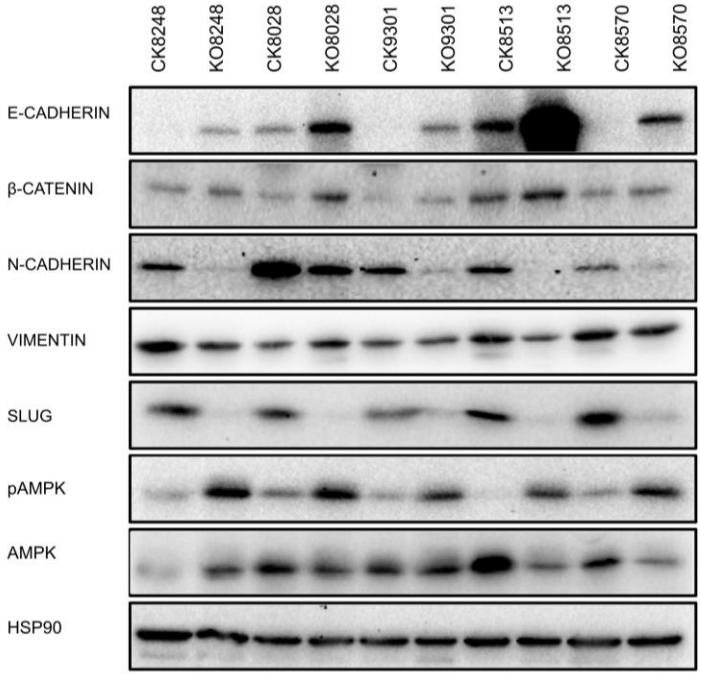
CK8248
KO8248
CK8028
KO8028
CK9301
KO9301
CK8513
KO8513
CK8570
KO8570
E-CADHERIN
β-CATENIN
N-CADHERIN
VIMENTIN
SLUG
pAMPK
AMPK
HSP90

D.

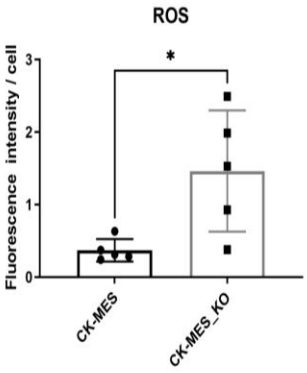
ROS
Fluorescence intensity / cell
3
2
1
0
*
CK-MES
CK-MES_KO

Figure III.5: *Txnrd2*-deficient pool generation and expression of EMT markers.

(A) The generated *Txnrd2*-deficient pool was validated by Western blot analysis. Total 5 pools were subjected into the validation.

(B) Enzymatic activity of TXNRD2 as determined by thioredoxin reductase assay in *Txnrd2*-deficient cells and control cells. Data are expressed using mean ± SD. Statistical results shown here by *($p < 0.05$).

(C) Protein expression of E-CADHERIN, VIMENTIN, β-CATENIN, N-CADHERiN, SLUG and pAMPK/AMPK as determined by Western blotting in 5 *Txnrd2*-deficient CK-MES cells. Hsp90 served as a loading control.

(D) ROS levels was determined by CellROX Green in *Txnrd2*-deficient CK-MES cells (n = 5) compared to *Txnrd2*-proficient CK-MES cells (n = 5). The results were normalized to cell number and data are expressed using mean ± SD. Statistical results shown here by *($p < 0.05$).

III.6. Deletion of *Txnrd2* repressed progression of CK-MES cells

Since the proliferation and migration ablities of CK-MES cells were repressed after the inhibition of TXNRD2 by Auranofin, we set out to determine the functional effect after *Txnrd2* deletion. In line with the results of Auranofin treatment, the proliferative rate of *Txnrd2*-deficient CK-MES was 15% lower than the *Txnrd2*-proficient CK-MES cells (Figure III.6A and III.6B). In addition, the colony formation capacity was significantly suppressed to 27.6% when *Txnrd2* was deleted in CK-MES cells (Figure III.6C and III.6D). The cell migration ability was also evaluated in CK-MES cells with different *Txnrd2* status. The migration ability was largely restricted in CK-MES_KO cells compared to CK-MES cells (Figure III.6E). In summary, *Txnrd2*-deficient CK-MES cells display a repressed ability of proliferation, colony formation and cell migration. Therefore deletion of *Txnrd2* represses proliferation and migration abilities of pancreatic cancer cells.

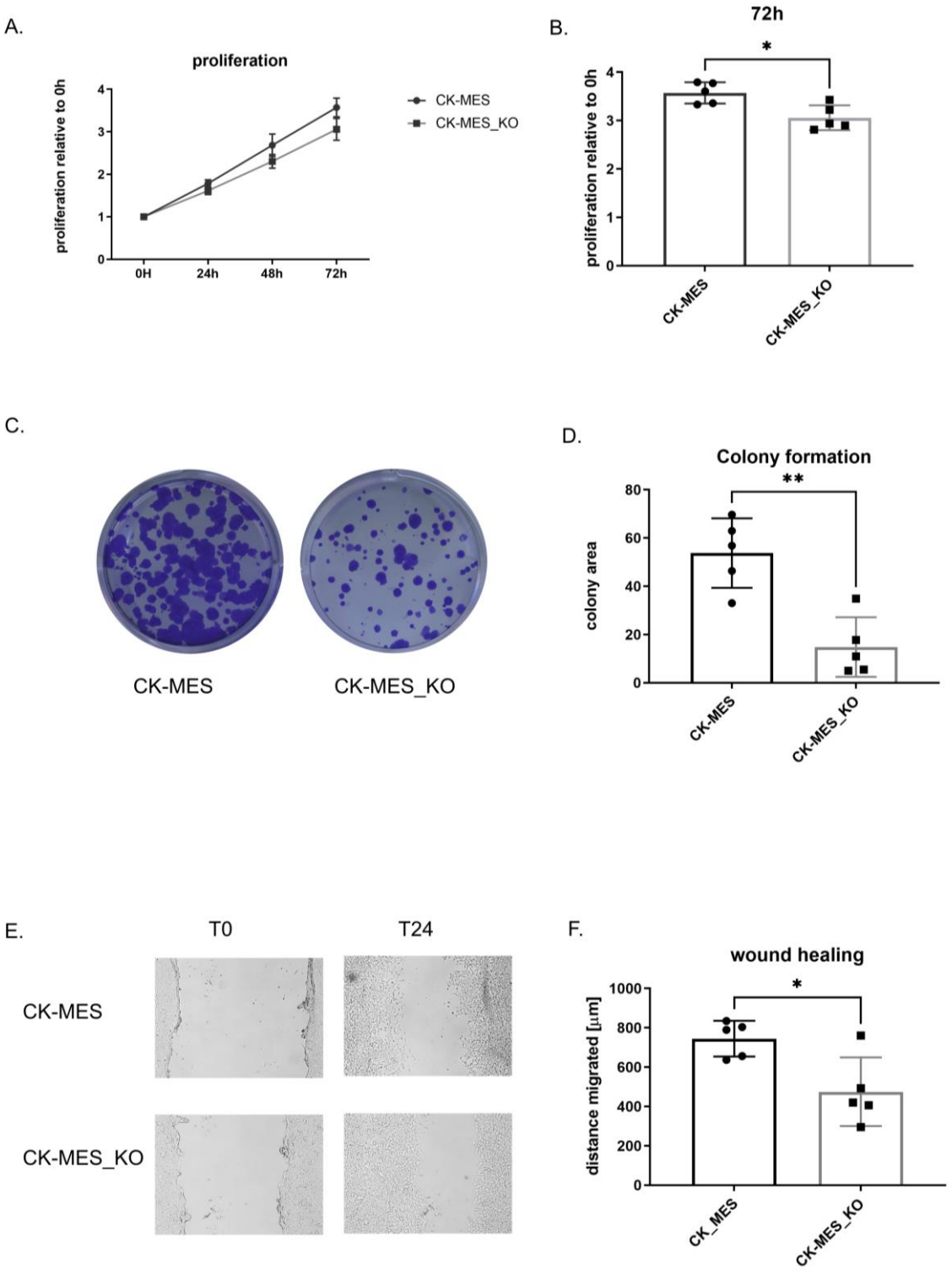

Figure III.6: Impaired proliferation, colony formation, and migration ability in the after the deletion of *Txnrd2* by CRISPR/Cas9.

(A) The proliferation of CK-MES KO cells was evaluated by CyQuant Assay after

incubated for up to 72 h. The results of each time point were normalized to the result of time point 0 h. Data are expressed using mean ± SD. Statistical results shown here by ns ($p \geq 0.05$), *($p < 0.05$), ** ($p < 0.01$), *** ($p < 0.001$)

(B) The proliferation of CK-MES (n = 5) and CK-MES KO (n = 5) cell lines was evaluated by CyQuant Assay at 72 h. The result of 72 h was normalized to the result of 0 h. Data are expressed using mean ± SD. Statistical results shown here by *($p < 0.05$).

(C) The colony capacity of CK-MES and CK-MES KO cells was evaluated by a colony formation assay after incubation of 1 week. The representative pictures of colony formation assay are shown in (C). Quantification of colony formation assay is presented in (D). Data are expressed using mean ± SD. Statistical results shown here by ** ($p < 0.01$).

(E) The migration ability of CK-MES and CK-MES KO cells was evaluated by a scratch assay. The representative pictures of scratch assay are shown in (E). Quantification of colony formation assay is presented in (F). Data are expressed using mean ± SD. Statistical results shown here by * ($p < 0.05$).

III.7. The effect of Re-expressing Txnrd2 in *Kras*^{G12D}; *Txnrd2*$^{\Delta Panc}$ cells

Primary *Txnrd2*-deficient cells from LSL-*Kras*$^{G12D/+}$; *Ptf1a*$^{Cre/+}$; *Txnrd2*$^{fl/fl}$ mice (Figure III.7A) were used. KTP19, 411715, 411869 and 410506 primary cell lines had been generated previously and the expression of TXNRD2 in all of these cells were validated by western blot analysis. The protein expression of TXNRD2 was absent in these four cell lines (Figure III.7B). To reintroduce the expression of TXNRD2, a Doxycycline (DOX)-induced *Txnrd2* vector was introduced by Lentivirus into cells derived from the *Txnrd2* KO mice. Cells with stable vectors were selected through treating infected cells with puromycin. The enzymic activity of TXNRD2 was increased in *Txnrd2*-deficient cells after ectopically expressed TXNRD2 by DOX (Figure III.7C). Western blot analysis demonstrated that TXNRD2 was induced by DOX treatment in all four *Txnrd2*-deficient cells (Figure III.7D). Furthermore, rescuing TXNRD2 repressed the phosphorylation of AMPK in *Txnrd2*-deficient cells (Figure III.7D), but the level of total AMPK was comparable before and after rescuing TXNRD2 in these cells (Figure III.7D). In addition, the expression of E-cadherin was repressed after TXNRD2 was reintroduced in *Txnrd2*-deficient cells, whereas the expression of N-cadherin was induced by reintroducing TXNRD2 in *Txnrd2*-deficient cells (Figure III.7D). Therefore, reintroducing TXNRD2 is capable of suppressing AMPK pathway and promoting EMT process in *Txnrd2*-deficient cells.

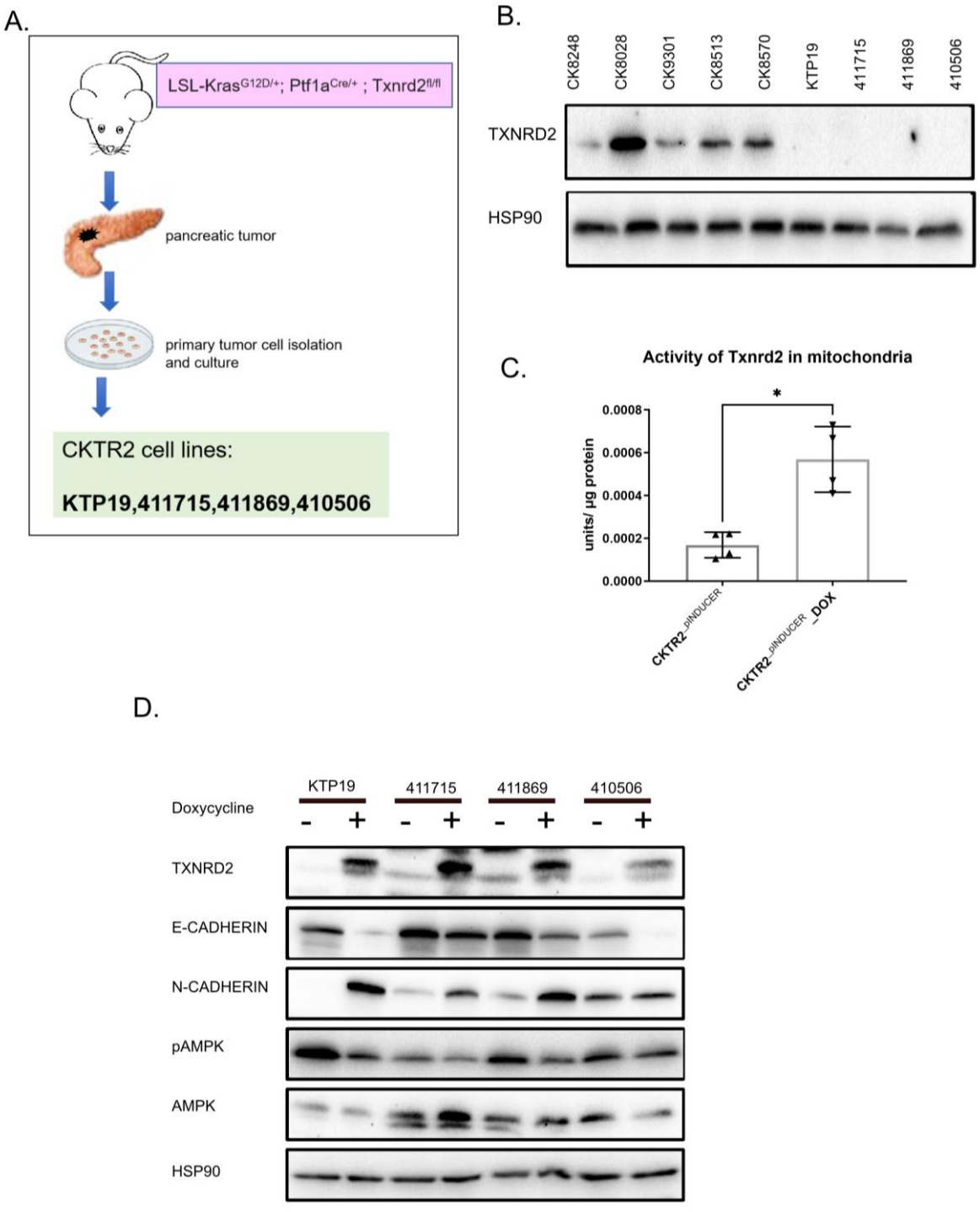

Figure III.7: Re-induce TXNRD2 expression on *Kras*^{G12D}; *Txnrd2*$^{\Delta\ panc}$ cell lines

(A) The pipeline of derivation of genetic *Txnrd2*-deficient cell lines from LSL-*Kras*$^{G12D/+}$; *Ptf1a*$^{Cre/+}$; *Txnrd2*$^{fl/fl}$ mice.

(B) The deficiency of TXNRD2 protein expression was validated by Western blotting in

the indicated derivated *Txnrd2*-deficient cells (KTP19, 411715, 411869 and 410506). HSP90 served as a loading control.

(C) Enzymatic activity of TXNRD2 in four derived *Txnrd2*-deficient cells with/without ectopic TXNRD2 induced by Doxycycline as determined by thioredoxin reductase assay. Data are expressed using mean ± SD. Statistical results shown here by *($p < 0.05$).

(D) The expression of EMT markers and pAMPK/AMPK was evaluated by western blotting in four *Txnrd2*-deficient cell lines with/without ectopic TXNRD2 induced by Doxycycline treatment. HSP90 served as a loading control.

IV. DISCUSSION

Accumulating evidence supports that thioredoxin (TRX) system is involved in the maintenance of EMT signaling and cancer progression (Faheem et al., 2020). TRX orchestrates the regulation of redox homeostasis in cells. Two isoforms of TRX have been identified in mammalian cells, namely cytosolic TXNRD1 and mitochondrial TXNRD2. Many studies demonstrate that TXNRD1 constitutes cell proliferation, cell cycle progression and angiogenesis (Arai et al., 2006; Arai et al., 2008; Farina et al., 2001; Nakamura et al., 1992). Typically, TXNRD1 is highly expressed in human primary cancers including in pancreatic cancer (Nakamura et al., 2000). Nevertheless, the expression of TXNRD1 was comparable in mesenchymal cells and epithelial cells in our study. Therefore, it appears to be the case that cellular morphology is independent of TXNRD1 expression.

As a core system of controlling cellular redox signaling and homeostasis, TRX is responsible for the regulation of reactive oxygen species (ROS) and associated pathways in cancer cells (Arner, 2017; Watson, 2013). TXNRD1 is a central regulator of TRX system. TXNRD1 is a cytosolic protein that is capable of catalyzing disulfide reduction in different substrates. Several oxidative posttranslational modifications also require TXNRD1 (Peng et al., 2016). Therefore, TXNRD1 is important for redox regulatory functions. The enzymatic functions of TXNRD1 largely rely on its Selenocysteine (Sec) residue that reduces the active disulfide of TXNRD1 to a dithiol (Stafford et al., 2018). Interestingly, glutaredoxins act in parallel with TXNRD1 and have partial overlapping functions. Indeed, the effector proteins of TXNRD1 and GSH systems have redundant functions in control of cell cycle and DNA precursor synthesis. Targeting GSH system may also repress TXNRD1 thereby causing cytotoxicity or tissue damage (Hayes et al., 2020). In addition, cytosolic glutaredoxin helps maintain

the reduced state of TXNRD1 by using GSH, which normalizes apoptosis pathways (Berndt et al., 2007). Multiple pharmacological approaches have been developed to kill cancer cells selectively by repressing TXNRD1 (Anestal et al., 2008; Arner, 2017; Becker et al., 2000; Cebula et al., 2015; Fang et al., 2005; Stafford et al., 2018; Wang et al., 2012; B. Zhang et al., 2017).

On the other hand, the antioxidant defense system mainly relies on mitochondrial peroxiredoxin (PRX3), which in turn is maintained by TXNRD2 in mitochondria (Cox et al., 2009; Rabilloud et al., 2001). TXNRD2 contains mitochondrial targeting sequence, thereby has a mitochondrial isoform (Miranda-Vizuete et al., 1999). In addition, TXNRD2 contains alternative splicing sites at the 5'-end, which generates two other transcripts coding cytosolic TXNRD2 isoforms without mitochondrial targeting sequence (Sun et al., 2001). Interestingly, the structure of TXNRD2 is similar to the cytosolic TXNRD1 (Gencheva & Arner, 2022), implying that they could be repressed by common inhibitors. In this study, only TXNRD2 protein level was increased in CK-MES cells compared to CK-EPI cells, whereas the expression of TXNRD1 mRNA was comparable in the two cell types. Furthermore, the enzymatic activity of TXNRD2 was enhanced significantly in mesenchymal cells. Some of the antioxidant proteins including GSTT2, GPX8 and SOD2 were also increased in CK-MES cells compared to CK-EPI cells, indicating a possible reduction in ROS levels relative to epithelial cells. Our observations suggest that TXNRD2, among other antioxidants, might be a vital player that modulates EMT.

Interestingly, ROS are often considered as EMT inducers due to their effect in regulation of transcription factors such as AP-1, HIF-1α, HSF1, NF-κB and p53. These transcription factors subsequently affect EMT-related transcription factors (Marinho et al., 2014). In this study, we show that knockdown of *Txnrd2* in CK-MES cells displayed

reversal of EMT characteristics as epithelial marker E-CADHERIN was increased and mesenchymal markers such as VIMENTIN, SLUG and N-CADHERIN were repressed as evaluated by western blot. Our results also showed that the ROS levels are significantly higher in CK-EPI cells compared to CK-MES cells. Moreover, ROS levels increased following *Txnrd2* deletion. Therefore, we hypothesize that TXNRD2-mediated ROS regulation might be involved in the promotion of EMT in pancreatic cancer. Previous studies indicate that EMT can be repressed by high ROS levels: The EMT-TF ZEB1 is repressed by the miR-200c that increases UTMD and ROS in breast cancer (Shi et al., 2020). These findings suggest that ROS might also be involved in the regulation of EMT process via TXNRD2-independent mechanisms.

In addition, previous studies show that increased expression of TXNRD2 promotes tumor growth and protects tumor cells from oxidative stress (Arner & Holmgren, 2006; Hayes et al., 2020). High levels of ROS induce DNA damage and protein oxidation which in turn trigger necrosis and apoptosis (Ott et al., 2007). Since TXNRD2 functions as an antioxidant, TXNRD2 may induce tumor growth through anti-apoptotic activity via repressing ROS. EMT was induced by TXNRD2 in isolated murine pancreatic cancer cells from LSL-*Kras*$^{G12D/+}$; *Ptf1a*$^{Cre/+}$; *Txnrd2*$^{fl/fl}$ mice in our study. However, a study on NMuMG mouse mammary epithelial cells showed that overexpression of TXNRD2 impairs the expression of fibronectin and AT-hook 2 protein, both of which are EMT markers and promote metastasis (Ishikawa et al., 2014). This indicates that the function of TXNRD2 in EMT regulation might be organ specific.

Here, by repressing TXNRD2, the AMPK pathway was activated. AMPK is a type of energy sensor in cells, that is activated when AMP and ADP increase due to the changes of ATP, ADP and AMP concentration in cells (Hardie, 2011b). The validation of ATP, ADP and AMP concentration is warranted to support AMPK activation after

TXNRD2 repression in the future study. The catalytic subunits of AMPK have a conventional Ser/Thr kinase domain (Suter et al., 2006). LKB1-STRAD-MO25 complex (Hawley et al., 2003; Shaw et al., 2004; Woods et al., 2003) and Ca^{2+}/calmodulin-activated protein kinase kinase (CaMKKs) (Hawley et al., 2005; Hurley et al., 2005; Woods et al., 2005) activate AMPK as up-stream kinases. In mammalian cells, AMPK is activated by multiple factors including metabolic stress and xenobiotics through aforementioned kinases, which refers to the classical or canonical AMPK activation. Studies indicate that AMPK is also activated by cellular stresses in a non-canonical way that the levels of AMP/ATP or Ca^{2+} is indifferent (Hardie, 2011a; Hardie et al., 2012). With AMPK activation, the production of ATP is increased following the enhanced expression or activity of catabolism proteins. However, the consumption of ATP is repressed due to the shutting down of biosynthetic pathways (Hardie et al., 2012). Previous studies have shown that AMPK is activated by ROS (Mungai et al., 2011; Zhao et al., 2017). Therefore, the activated AMPK is possibly caused by the increased ROS levels due to the repression of TXNRD2 in our study.

Activation of AMPK triggers the response of antioxidants relying on PGC-1α, and the mitochondrial ROS are subsequently limited (St-Pierre et al., 2006), which indicates AMPK and ROS form a feedback loop in the regulation of cellular metabolic balance. In CK-MES cells with high TXNRD2 level, several antioxidants were also elevated, whereas the ROS levels were decreased. However, this warrants further investigation.

Furthermore, AMPK appears to be a tumor suppressor by inhibiting EMT in different cancers (Kullmann & Krahn, 2018; Penugurti et al., 2022; Ponnusamy et al., 2020). Knockdown of AMPK reduces the expression of FOXO3A and E-CADHERIN whereas the expression of VIMENTIN and SNAI1 is increased, which induces EMT in breast and prostate cancers (Chou et al., 2014). Inactivation of AMPK confers cancer stem

cell-like properties to epithelial cells, which leads to breaching of the basement membrane and metastasis to distant sites (Chou et al., 2014). In this study, AMPK was activated in *Txnrd2*-deficient cells, therefore, AMPK may mediate the effects of TXNRD2 deletion observed in our model. However, this hypothesis has to be tested using AMPK activation and inhibition experiments.

Additionally, we induced functional TXNRD2 in *Txnrd2*-deficient cells through lentiviral transduction and doxycycline treatment. In line with our findings so far, we observed that TXNRD2 reinduction results in repression of epithelial marker E-CADHERIN and increase of expression of mesenchymal marker N-CADHERIN. Interestingly, we observed a concomitant decrease in phosphorylated AMPK. This clearly indicates that TXNRD2 is a key player in regulation of EMT process via redox modulation.

V. Conclusion

TXNRD2 is positively associated with mesenchymal phenotype in pancreatic cancer cells. Cell proliferation, colony formation capacity and mesenchymal characteristics are repressed when TXNRD2 is pharmacologically inhibited or genetically knocked down. As a regulator of redox balance, repression or reinduction of TXNRD2 modulates ROS levels, which seems to be a potential mechanism involved in the regulation of EMT in pancreatic cancer.

VI. References

Aguirre, A. J., Bardeesy, N., Sinha, M., Lopez, L., Tuveson, D. A., Horner, J., Redston, M. S., & DePinho, R. A. (2003). Activated Kras and Ink4a/Arf deficiency cooperate to produce metastatic pancreatic ductal adenocarcinoma. *Genes Dev*, *17*(24), 3112-3126. https://doi.org/10.1101/gad.1158703

Ahmed, S., Bradshaw, A. D., Gera, S., Dewan, M. Z., & Xu, R. (2017). The TGF-beta/Smad4 Signaling Pathway in Pancreatic Carcinogenesis and Its Clinical Significance. *J Clin Med*, *6*(1). https://doi.org/10.3390/jcm6010005

Anestal, K., Prast-Nielsen, S., Cenas, N., & Arner, E. S. (2008). Cell death by SecTRAPs: thioredoxin reductase as a prooxidant killer of cells. *PLoS One*, *3*(4), e1846. https://doi.org/10.1371/journal.pone.0001846

Arai, R. J., Masutani, H., Yodoi, J., Debbas, V., Laurindo, F. R., Stern, A., & Monteiro, H. P. (2006). Nitric oxide induces thioredoxin-1 nuclear translocation: possible association with the p21Ras survival pathway. *Biochem Biophys Res Commun*, *348*(4), 1254-1260. https://doi.org/10.1016/j.bbrc.2006.07.178

Arai, R. J., Ogata, F. T., Batista, W. L., Masutani, H., Yodoi, J., Debbas, V., Augusto, O., Stern, A., & Monteiro, H. P. (2008). Thioredoxin-1 promotes survival in cells exposed to S-nitrosoglutathione: Correlation with reduction of intracellular levels of nitrosothiols and up-regulation of the ERK1/2 MAP Kinases. *Toxicol Appl Pharmacol*, *233*(2), 227-237. https://doi.org/10.1016/j.taap.2008.07.023

Arner, E. S., & Holmgren, A. (2006). The thioredoxin system in cancer. *Semin Cancer Biol*, *16*(6), 420-426. https://doi.org/10.1016/j.semcancer.2006.10.009

Arner, E. S. J. (2017). Targeting the Selenoprotein Thioredoxin Reductase 1 for Anticancer Therapy. *Adv Cancer Res*, *136*, 139-151. https://doi.org/10.1016/bs.acr.2017.07.005

Arnold, N. B., Ketterer, K., Kleeff, J., Friess, H., Buchler, M. W., & Korc, M. (2004). Thioredoxin is downstream of Smad7 in a pathway that promotes growth and suppresses cisplatin-induced apoptosis in pancreatic cancer. *Cancer Res*, *64*(10), 3599-3606. https://doi.org/10.1158/0008-5472.CAN-03-2999

Becker, K., Gromer, S., Schirmer, R. H., & Muller, S. (2000). Thioredoxin reductase as a pathophysiological factor and drug target. *Eur J Biochem*, *267*(20), 6118-6125. https://doi.org/10.1046/j.1432-1327.2000.01703.x

Benhar, M., Shytaj, I. L., Stamler, J. S., & Savarino, A. (2016). Dual targeting of the thioredoxin and glutathione systems in cancer and HIV. *J Clin Invest*, *126*(5), 1630-1639. https://doi.org/10.1172/JCI85339

Berndt, C., Hudemann, C., Hanschmann, E. M., Axelsson, R., Holmgren, A., & Lillig, C. H. (2007). How does iron-sulfur cluster coordination regulate the activity of human glutaredoxin 2? *Antioxid Redox Signal*, *9*(1), 151-157. https://doi.org/10.1089/ars.2007.9.151

Bhatia, M., McGrath, K. L., Di Trapani, G., Charoentong, P., Shah, F., King, M. M., Clarke, F. M., & Tonissen, K. F. (2016). The thioredoxin system in breast cancer cell invasion and migration. *Redox Biol*, *8*, 68-78. https://doi.org/10.1016/j.redox.2015.12.004

Blackford, A. L., Canto, M. I., Klein, A. P., Hruban, R. H., & Goggins, M. (2020). Recent Trends in the Incidence and Survival of Stage 1A Pancreatic Cancer: A Surveillance, Epidemiology, and End Results Analysis. *J Natl Cancer Inst*, *112*(11), 1162-1169. https://doi.org/10.1093/jnci/djaa004

Bon, H., Wadhwa, K., Schreiner, A., Osborne, M., Carroll, T., Ramos-Montoya, A., Ross-Adams, H., Visser, M., Hoffmann, R., Ahmed, A. A., Neal, D. E., & Mills, I. G. (2015). Salt-inducible kinase 2 regulates mitotic progression and

transcription in prostate cancer. *Mol Cancer Res*, *13*(4), 620-635. https://doi.org/10.1158/1541-7786.MCR-13-0182-T

Bosetti, C., Lucenteforte, E., Silverman, D. T., Petersen, G., Bracci, P. M., Ji, B. T., Negri, E., Li, D., Risch, H. A., Olson, S. H., Gallinger, S., Miller, A. B., Bueno-de-Mesquita, H. B., Talamini, R., Polesel, J., Ghadirian, P., Baghurst, P. A., Zatonski, W., Fontham, E., Bamlet, W. R., Holly, E. A., Bertuccio, P., Gao, Y. T., Hassan, M., Yu, H., Kurtz, R. C., Cotterchio, M., Su, J., Maisonneuve, P., Duell, E. J., Boffetta, P., & La Vecchia, C. (2012). Cigarette smoking and pancreatic cancer: an analysis from the International Pancreatic Cancer Case-Control Consortium (Panc4). *Ann Oncol*, *23*(7), 1880-1888. https://doi.org/10.1093/annonc/mdr541

Bosetti, C., Rosato, V., Li, D., Silverman, D., Petersen, G. M., Bracci, P. M., Neale, R. E., Muscat, J., Anderson, K., Gallinger, S., Olson, S. H., Miller, A. B., Bas Bueno-de-Mesquita, H., Scelo, G., Janout, V., Holcatova, I., Lagiou, P., Serraino, D., Lucenteforte, E., Fabianova, E., Baghurst, P. A., Zatonski, W., Foretova, L., Fontham, E., Bamlet, W. R., Holly, E. A., Negri, E., Hassan, M., Prizment, A., Cotterchio, M., Cleary, S., Kurtz, R. C., Maisonneuve, P., Trichopoulos, D., Polesel, J., Duell, E. J., Boffetta, P., La Vecchia, C., & Ghadirian, P. (2014). Diabetes, antidiabetic medications, and pancreatic cancer risk: an analysis from the International Pancreatic Cancer Case-Control Consortium. *Ann Oncol*, *25*(10), 2065-2072. https://doi.org/10.1093/annonc/mdu276

Bradshaw, P. C. (2019). Cytoplasmic and Mitochondrial NADPH-Coupled Redox Systems in the Regulation of Aging. *Nutrients*, *11*(3). https://doi.org/10.3390/nu11030504

Cairns, J. (1975). Mutation selection and the natural history of cancer. *Nature*, *255*(5505), 197-200. https://doi.org/10.1038/255197a0

Calle, E. E., Rodriguez, C., Walker-Thurmond, K., & Thun, M. J. (2003). Overweight, obesity, and mortality from cancer in a prospectively studied cohort of U.S. adults. *N Engl J Med*, *348*(17), 1625-1638. https://doi.org/10.1056/NEJMoa021423

Campbell, P. J., Yachida, S., Mudie, L. J., Stephens, P. J., Pleasance, E. D., Stebbings, L. A., Morsberger, L. A., Latimer, C., McLaren, S., Lin, M. L., McBride, D. J., Varela, I., Nik-Zainal, S. A., Leroy, C., Jia, M., Menzies, A., Butler, A. P., Teague, J. W., Griffin, C. A., Burton, J., Swerdlow, H., Quail, M. A., Stratton, M. R., Iacobuzio-Donahue, C., & Futreal, P. A. (2010). The patterns and dynamics of genomic instability in metastatic pancreatic cancer. *Nature*, *467*(7319), 1109-1113. https://doi.org/10.1038/nature09460

Cebula, M., Schmidt, E. E., & Arner, E. S. (2015). TrxR1 as a potent regulator of the Nrf2-Keap1 response system. *Antioxid Redox Signal*, *23*(10), 823-853. https://doi.org/10.1089/ars.2015.6378

Cenas, N., Nivinskas, H., Anusevicius, Z., Sarlauskas, J., Lederer, F., & Arner, E. S. (2004). Interactions of quinones with thioredoxin reductase: a challenge to the antioxidant role of the mammalian selenoprotein. *J Biol Chem*, *279*(4), 2583-2592. https://doi.org/10.1074/jbc.M310292200

Chandra, D., & Singh, K. K. (2011). Genetic insights into OXPHOS defect and its role in cancer. *Biochim Biophys Acta*, *1807*(6), 620-625. https://doi.org/10.1016/j.bbabio.2010.10.023

Chatterjee, R., & Chatterjee, J. (2020). ROS and oncogenesis with special reference to EMT and stemness. *Eur J Cell Biol*, *99*(2-3), 151073. https://doi.org/10.1016/j.ejcb.2020.151073

Chen, Y. W., Hsiao, P. J., Weng, C. C., Kuo, K. K., Kuo, T. L., Wu, D. C., Hung, W. C., & Cheng, K. H. (2014). SMAD4 loss triggers the phenotypic changes of pancreatic ductal adenocarcinoma cells. *BMC Cancer*, *14*, 181. https://doi.org/10.1186/1471-2407-14-181

Chou, C. C., Lee, K. H., Lai, I. L., Wang, D., Mo, X., Kulp, S. K., Shapiro, C. L., & Chen, C. S. (2014). AMPK reverses the mesenchymal phenotype of cancer cells by targeting the Akt-MDM2-Foxo3a signaling axis. *Cancer Res*, *74*(17), 4783-4795. https://doi.org/10.1158/0008-5472.CAN-14-0135

Chouat, E., Zehani, A., Chelly, I., Njima, M., Maghrebi, H., Bani, M. A., Njim, L., Zakhama, A., Haouet, S., & Kchir, N. (2018). Tumor budding is a prognostic factor linked to epithelial mesenchymal transition in pancreatic ductal adenocarcinoma. Study report and literature review. *Pancreatology*, *18*(1), 79-84. https://doi.org/10.1016/j.pan.2017.11.010

Chung, C. T., & Miller, R. H. (1988). A rapid and convenient method for the preparation and storage of competent bacterial cells. *Nucleic Acids Res*, *16*(8), 3580. https://doi.org/10.1093/nar/16.8.3580

Collaborators, G. B. D. P. C. (2019). The global, regional, and national burden of pancreatic cancer and its attributable risk factors in 195 countries and territories, 1990-2017: a systematic analysis for the Global Burden of Disease Study 2017. *Lancet Gastroenterol Hepatol*, *4*(12), 934-947. https://doi.org/10.1016/S2468-1253(19)30347-4

Collins, M. A., Bednar, F., Zhang, Y., Brisset, J. C., Galban, S., Galban, C. J., Rakshit, S., Flannagan, K. S., Adsay, N. V., & Pasca di Magliano, M. (2012). Oncogenic Kras is required for both the initiation and maintenance of pancreatic cancer in mice. *J Clin Invest*, *122*(2), 639-653. https://doi.org/10.1172/JCI59227

Collisson, E. A., Sadanandam, A., Olson, P., Gibb, W. J., Truitt, M., Gu, S., Cooc, J., Weinkle, J., Kim, G. E., Jakkula, L., Feiler, H. S., Ko, A. H., Olshen, A. B., Danenberg, K. L., Tempero, M. A., Spellman, P. T., Hanahan, D., & Gray, J. W. (2011). Subtypes of pancreatic ductal adenocarcinoma and their differing responses to therapy. *Nat Med*, *17*(4), 500-503. https://doi.org/10.1038/nm.2344

Cox, A. G., Winterbourn, C. C., & Hampton, M. B. (2009). Mitochondrial peroxiredoxin involvement in antioxidant defence and redox signalling. *Biochem J*, *425*(2), 313-325. https://doi.org/10.1042/BJ20091541

Dai, C., Rennhack, J. P., Arnoff, T. E., Thaker, M., Younger, S. T., Doench, J. G., Huang, A. Y., Yang, A., Aguirre, A. J., Wang, B., Mun, E., O'Connell, J. T., Huang, Y., Labella, K., Talamas, J. A., Li, J., Ilic, N., Hwang, J., Hong, A. L., Giacomelli, A. O., Gjoerup, O., Root, D. E., & Hahn, W. C. (2021). SMAD4 represses FOSL1 expression and pancreatic cancer metastatic colonization. *Cell Rep*, *36*(4), 109443. https://doi.org/10.1016/j.celrep.2021.109443

Delitto, D., Zhang, D., Han, S., Black, B. S., Knowlton, A. E., Vlada, A. C., Sarosi, G. A., Behrns, K. E., Thomas, R. M., Lu, X., Liu, C., George, T. J., Hughes, S. J., Wallet, S. M., & Trevino, J. G. (2016). Nicotine Reduces Survival via Augmentation of Paracrine HGF-MET Signaling in the Pancreatic Cancer Microenvironment. *Clin Cancer Res*, *22*(7), 1787-1799. https://doi.org/10.1158/1078-0432.CCR-15-1256

Dodson, M., Castro-Portuguez, R., & Zhang, D. D. (2019). NRF2 plays a critical role in mitigating lipid peroxidation and ferroptosis. *Redox Biol*, *23*, 101107. https://doi.org/10.1016/j.redox.2019.101107

Du, Y., Zhang, H., Lu, J., & Holmgren, A. (2012). Glutathione and glutaredoxin act as a backup of human thioredoxin reductase 1 to reduce thioredoxin 1 preventing

cell death by aurothioglucose. *J Biol Chem*, *287*(45), 38210-38219. https://doi.org/10.1074/jbc.M112.392225

Ducreux, M., Cuhna, A. S., Caramella, C., Hollebecque, A., Burtin, P., Goere, D., Seufferlein, T., Haustermans, K., Van Laethem, J. L., Conroy, T., Arnold, D., & Committee, E. G. (2015). Cancer of the pancreas: ESMO Clinical Practice Guidelines for diagnosis, treatment and follow-up. *Ann Oncol*, *26 Suppl 5*, v56-68. https://doi.org/10.1093/annonc/mdv295

Duell, E. J., Lucenteforte, E., Olson, S. H., Bracci, P. M., Li, D., Risch, H. A., Silverman, D. T., Ji, B. T., Gallinger, S., Holly, E. A., Fontham, E. H., Maisonneuve, P., Bueno-de-Mesquita, H. B., Ghadirian, P., Kurtz, R. C., Ludwig, E., Yu, H., Lowenfels, A. B., Seminara, D., Petersen, G. M., La Vecchia, C., & Boffetta, P. (2012). Pancreatitis and pancreatic cancer risk: a pooled analysis in the International Pancreatic Cancer Case-Control Consortium (PanC4). *Ann Oncol*, *23*(11), 2964-2970. https://doi.org/10.1093/annonc/mds140

Elena, J. W., Steplowski, E., Yu, K., Hartge, P., Tobias, G. S., Brotzman, M. J., Chanock, S. J., Stolzenberg-Solomon, R. Z., Arslan, A. A., Bueno-de-Mesquita, H. B., Helzlsouer, K., Jacobs, E. J., LaCroix, A., Petersen, G., Zheng, W., Albanes, D., Allen, N. E., Amundadottir, L., Bao, Y., Boeing, H., Boutron-Ruault, M. C., Buring, J. E., Gaziano, J. M., Giovannucci, E. L., Duell, E. J., Hallmans, G., Howard, B. V., Hunter, D. J., Hutchinson, A., Jacobs, K. B., Kooperberg, C., Kraft, P., Mendelsohn, J. B., Michaud, D. S., Palli, D., Phillips, L. S., Overvad, K., Patel, A. V., Sansbury, L., Shu, X. O., Simon, M. S., Slimani, N., Trichopoulos, D., Visvanathan, K., Virtamo, J., Wolpin, B. M., Zeleniuch-Jacquotte, A., Fuchs, C. S., Hoover, R. N., & Gross, M. (2013). Diabetes and risk of pancreatic cancer: a pooled analysis from the pancreatic cancer cohort

consortium. *Cancer Causes Control*, *24*(1), 13-25. https://doi.org/10.1007/s10552-012-0078-8

Eriksson, S. E., Prast-Nielsen, S., Flaberg, E., Szekely, L., & Arner, E. S. (2009). High levels of thioredoxin reductase 1 modulate drug-specific cytotoxic efficacy. *Free Radic Biol Med*, *47*(11), 1661-1671. https://doi.org/10.1016/j.freeradbiomed.2009.09.016

Everhart, J., & Wright, D. (1995). Diabetes mellitus as a risk factor for pancreatic cancer. A meta-analysis. *JAMA*, *273*(20), 1605-1609. https://www.ncbi.nlm.nih.gov/pubmed/7745774

Faheem, M. M., Seligson, N. D., Ahmad, S. M., Rasool, R. U., Gandhi, S. G., Bhagat, M., & Goswami, A. (2020). Convergence of therapy-induced senescence (TIS) and EMT in multistep carcinogenesis: current opinions and emerging perspectives. *Cell Death Discov*, *6*, 51. https://doi.org/10.1038/s41420-020-0286-z

Fan, X., Alekseyenko, A. V., Wu, J., Peters, B. A., Jacobs, E. J., Gapstur, S. M., Purdue, M. P., Abnet, C. C., Stolzenberg-Solomon, R., Miller, G., Ravel, J., Hayes, R. B., & Ahn, J. (2018). Human oral microbiome and prospective risk for pancreatic cancer: a population-based nested case-control study. *Gut*, *67*(1), 120-127. https://doi.org/10.1136/gutjnl-2016-312580

Fang, J., Lu, J., & Holmgren, A. (2005). Thioredoxin reductase is irreversibly modified by curcumin: a novel molecular mechanism for its anticancer activity. *J Biol Chem*, *280*(26), 25284-25290. https://doi.org/10.1074/jbc.M414645200

Farina, A. R., Tacconelli, A., Cappabianca, L., Masciulli, M. P., Holmgren, A., Beckett, G. J., Gulino, A., & Mackay, A. R. (2001). Thioredoxin alters the matrix metalloproteinase/tissue inhibitors of metalloproteinase balance and stimulates

human SK-N-SH neuroblastoma cell invasion. *Eur J Biochem*, *268*(2), 405-413. https://doi.org/10.1046/j.1432-1033.2001.01892.x

Faubert, B., Boily, G., Izreig, S., Griss, T., Samborska, B., Dong, Z., Dupuy, F., Chambers, C., Fuerth, B. J., Viollet, B., Mamer, O. A., Avizonis, D., DeBerardinis, R. J., Siegel, P. M., & Jones, R. G. (2013). AMPK is a negative regulator of the Warburg effect and suppresses tumor growth in vivo. *Cell Metab*, *17*(1), 113-124. https://doi.org/10.1016/j.cmet.2012.12.001

Font-Burgada, J., Sun, B., & Karin, M. (2016). Obesity and Cancer: The Oil that Feeds the Flame. *Cell Metab*, *23*(1), 48-62. https://doi.org/10.1016/j.cmet.2015.12.015

Gallo-Oller, G., Ordonez, R., & Dotor, J. (2018). A new background subtraction method for Western blot densitometry band quantification through image analysis software. *J Immunol Methods*, *457*, 1-5. https://doi.org/10.1016/j.jim.2018.03.004

Galvan, J. A., Zlobec, I., Wartenberg, M., Lugli, A., Gloor, B., Perren, A., & Karamitopoulou, E. (2015). Expression of E-cadherin repressors SNAIL, ZEB1 and ZEB2 by tumour and stromal cells influences tumour-budding phenotype and suggests heterogeneity of stromal cells in pancreatic cancer. *Br J Cancer*, *112*(12), 1944-1950. https://doi.org/10.1038/bjc.2015.177

Gapstur, S. M., Jacobs, E. J., Deka, A., McCullough, M. L., Patel, A. V., & Thun, M. J. (2011). Association of alcohol intake with pancreatic cancer mortality in never smokers. *Arch Intern Med*, *171*(5), 444-451. https://doi.org/10.1001/archinternmed.2010.536

Gencheva, R., & Arner, E. S. J. (2022). Thioredoxin Reductase Inhibition for Cancer Therapy. *Annu Rev Pharmacol Toxicol*, *62*, 177-196. https://doi.org/10.1146/annurev-pharmtox-052220-102509

Gillen, S., Schuster, T., Meyer Zum Buschenfelde, C., Friess, H., & Kleeff, J. (2010). Preoperative/neoadjuvant therapy in pancreatic cancer: a systematic review and meta-analysis of response and resection percentages. *PLoS Med*, *7*(4), e1000267. https://doi.org/10.1371/journal.pmed.1000267

Giovannetti, E., van der Borden, C. L., Frampton, A. E., Ali, A., Firuzi, O., & Peters, G. J. (2017). Never let it go: Stopping key mechanisms underlying metastasis to fight pancreatic cancer. *Semin Cancer Biol*, *44*, 43-59. https://doi.org/10.1016/j.semcancer.2017.04.006

Hardie, D. G. (2011a). AMP-activated protein kinase: an energy sensor that regulates all aspects of cell function. *Genes Dev*, *25*(18), 1895-1908. https://doi.org/10.1101/gad.17420111

Hardie, D. G. (2011b). Sensing of energy and nutrients by AMP-activated protein kinase. *Am J Clin Nutr*, *93*(4), 891S-896. https://doi.org/10.3945/ajcn.110.001925

Hardie, D. G., Ross, F. A., & Hawley, S. A. (2012). AMPK: a nutrient and energy sensor that maintains energy homeostasis. *Nat Rev Mol Cell Biol*, *13*(4), 251-262. https://doi.org/10.1038/nrm3311

Hawley, S. A., Boudeau, J., Reid, J. L., Mustard, K. J., Udd, L., Makela, T. P., Alessi, D. R., & Hardie, D. G. (2003). Complexes between the LKB1 tumor suppressor, STRAD alpha/beta and MO25 alpha/beta are upstream kinases in the AMP-activated protein kinase cascade. *J Biol*, *2*(4), 28. https://doi.org/10.1186/1475-4924-2-28

Hawley, S. A., Pan, D. A., Mustard, K. J., Ross, L., Bain, J., Edelman, A. M., Frenguelli, B. G., & Hardie, D. G. (2005). Calmodulin-dependent protein kinase kinase-beta is an alternative upstream kinase for AMP-activated protein kinase. *Cell Metab*, *2*(1), 9-19. https://doi.org/10.1016/j.cmet.2005.05.009

Hay, E. D. (2005). The mesenchymal cell, its role in the embryo, and the remarkable signaling mechanisms that create it. *Dev Dyn*, *233*(3), 706-720. https://doi.org/10.1002/dvdy.20345

Hayes, J. D., Dinkova-Kostova, A. T., & Tew, K. D. (2020). Oxidative Stress in Cancer. *Cancer Cell*, *38*(2), 167-197. https://doi.org/10.1016/j.ccell.2020.06.001

He, J., Ahuja, N., Makary, M. A., Cameron, J. L., Eckhauser, F. E., Choti, M. A., Hruban, R. H., Pawlik, T. M., & Wolfgang, C. L. (2014). 2564 resected periampullary adenocarcinomas at a single institution: trends over three decades. *HPB (Oxford)*, *16*(1), 83-90. https://doi.org/10.1111/hpb.12078

Hellman, S. (1994). Karnofsky Memorial Lecture. Natural history of small breast cancers. *J Clin Oncol*, *12*(10), 2229-2234. https://doi.org/10.1200/JCO.1994.12.10.2229

Hingorani, S. R., Wang, L., Multani, A. S., Combs, C., Deramaudt, T. B., Hruban, R. H., Rustgi, A. K., Chang, S., & Tuveson, D. A. (2005). Trp53R172H and KrasG12D cooperate to promote chromosomal instability and widely metastatic pancreatic ductal adenocarcinoma in mice. *Cancer Cell*, *7*(5), 469-483. https://doi.org/10.1016/j.ccr.2005.04.023

Hobbs, G. A., Der, C. J., & Rossman, K. L. (2016). RAS isoforms and mutations in cancer at a glance. *J Cell Sci*, *129*(7), 1287-1292. https://doi.org/10.1242/jcs.182873

Hotz, B., Arndt, M., Dullat, S., Bhargava, S., Buhr, H. J., & Hotz, H. G. (2007). Epithelial to mesenchymal transition: expression of the regulators snail, slug, and twist in pancreatic cancer. *Clin Cancer Res*, *13*(16), 4769-4776. https://doi.org/10.1158/1078-0432.CCR-06-2926

Hu, C., Hart, S. N., Polley, E. C., Gnanaolivu, R., Shimelis, H., Lee, K. Y., Lilyquist, J., Na, J., Moore, R., Antwi, S. O., Bamlet, W. R., Chaffee, K. G., DiCarlo, J., Wu,

Z., Samara, R., Kasi, P. M., McWilliams, R. R., Petersen, G. M., & Couch, F. J. (2018). Association Between Inherited Germline Mutations in Cancer Predisposition Genes and Risk of Pancreatic Cancer. *JAMA*, *319*(23), 2401-2409. https://doi.org/10.1001/jama.2018.6228

Hurley, R. L., Anderson, K. A., Franzone, J. M., Kemp, B. E., Means, A. R., & Witters, L. A. (2005). The Ca2+/calmodulin-dependent protein kinase kinases are AMP-activated protein kinase kinases. *J Biol Chem*, *280*(32), 29060-29066. https://doi.org/10.1074/jbc.M503824200

Huxley, R., Ansary-Moghaddam, A., Berrington de Gonzalez, A., Barzi, F., & Woodward, M. (2005). Type-II diabetes and pancreatic cancer: a meta-analysis of 36 studies. *Br J Cancer*, *92*(11), 2076-2083. https://doi.org/10.1038/sj.bjc.6602619

Iodice, S., Gandini, S., Maisonneuve, P., & Lowenfels, A. B. (2008). Tobacco and the risk of pancreatic cancer: a review and meta-analysis. *Langenbecks Arch Surg*, *393*(4), 535-545. https://doi.org/10.1007/s00423-007-0266-2

Ishikawa, F., Kaneko, E., Sugimoto, T., Ishijima, T., Wakamatsu, M., Yuasa, A., Sampei, R., Mori, K., Nose, K., & Shibanuma, M. (2014). A mitochondrial thioredoxin-sensitive mechanism regulates TGF-beta-mediated gene expression associated with epithelial-mesenchymal transition. *Biochem Biophys Res Commun*, *443*(3), 821-827. https://doi.org/10.1016/j.bbrc.2013.12.050

Jemal, A., Siegel, R., Ward, E., Murray, T., Xu, J., Smigal, C., & Thun, M. J. (2006). Cancer statistics, 2006. *CA Cancer J Clin*, *56*(2), 106-130. https://doi.org/10.3322/canjclin.56.2.106

Jiang, J., Wang, K., Chen, Y., Chen, H., Nice, E. C., & Huang, C. (2017). Redox regulation in tumor cell epithelial-mesenchymal transition: molecular basis and

therapeutic strategy. *Signal Transduct Target Ther*, *2*, 17036. https://doi.org/10.1038/sigtrans.2017.36

Jovanovic, M., Podolski-Renic, A., Krasavin, M., & Pesic, M. (2022). The Role of the Thioredoxin Detoxification System in Cancer Progression and Resistance. *Front Mol Biosci*, *9*, 883297. https://doi.org/10.3389/fmolb.2022.883297

Kalluri, R., & Weinberg, R. A. (2009). The basics of epithelial-mesenchymal transition. *J Clin Invest*, *119*(6), 1420-1428. https://doi.org/10.1172/JCI39104

Kanda, M., Matthaei, H., Wu, J., Hong, S. M., Yu, J., Borges, M., Hruban, R. H., Maitra, A., Kinzler, K., Vogelstein, B., & Goggins, M. (2012). Presence of somatic mutations in most early-stage pancreatic intraepithelial neoplasia. *Gastroenterology*, *142*(4), 730-733 e739. https://doi.org/10.1053/j.gastro.2011.12.042

Kang, Y., Ling, J., Suzuki, R., Roife, D., Chopin-Laly, X., Truty, M. J., Chatterjee, D., Wang, H., Thomas, R. M., Katz, M. H., Chiao, P. J., & Fleming, J. B. (2014). SMAD4 regulates cell motility through transcription of N-cadherin in human pancreatic ductal epithelium. *PLoS One*, *9*(9), e107948. https://doi.org/10.1371/journal.pone.0107948

Kim, M. P., Li, X., Deng, J., Zhang, Y., Dai, B., Allton, K. L., Hughes, T. G., Siangco, C., Augustine, J. J., Kang, Y., McDaniel, J. M., Xiong, S., Koay, E. J., McAllister, F., Bristow, C. A., Heffernan, T. P., Maitra, A., Liu, B., Barton, M. C., Wasylishen, A. R., Fleming, J. B., & Lozano, G. (2021). Oncogenic KRAS Recruits an Expansive Transcriptional Network through Mutant p53 to Drive Pancreatic Cancer Metastasis. *Cancer Discov*, *11*(8), 2094-2111. https://doi.org/10.1158/2159-8290.CD-20-1228

Kim, S. J., Miyoshi, Y., Taguchi, T., Tamaki, Y., Nakamura, H., Yodoi, J., Kato, K., & Noguchi, S. (2005). High thioredoxin expression is associated with resistance

to docetaxel in primary breast cancer. *Clin Cancer Res*, *11*(23), 8425-8430. https://doi.org/10.1158/1078-0432.CCR-05-0449

Kleeff, J., Korc, M., Apte, M., La Vecchia, C., Johnson, C. D., Biankin, A. V., Neale, R. E., Tempero, M., Tuveson, D. A., Hruban, R. H., & Neoptolemos, J. P. (2016). Pancreatic cancer. *Nat Rev Dis Primers*, *2*, 16022. https://doi.org/10.1038/nrdp.2016.22

Klein, A. P. (2021). Pancreatic cancer epidemiology: understanding the role of lifestyle and inherited risk factors. *Nat Rev Gastroenterol Hepatol*, *18*(7), 493-502. https://doi.org/10.1038/s41575-021-00457-x

Klein, C. A. (2009). Parallel progression of primary tumours and metastases. *Nat Rev Cancer*, *9*(4), 302-312. https://doi.org/10.1038/nrc2627

Kohler, I., Bronsert, P., Timme, S., Werner, M., Brabletz, T., Hopt, U. T., Schilling, O., Bausch, D., Keck, T., & Wellner, U. F. (2015). Detailed analysis of epithelial-mesenchymal transition and tumor budding identifies predictors of long-term survival in pancreatic ductal adenocarcinoma. *J Gastroenterol Hepatol*, *30 Suppl 1*, 78-84. https://doi.org/10.1111/jgh.12752

Koundouros, N., & Poulogiannis, G. (2018). Phosphoinositide 3-Kinase/Akt Signaling and Redox Metabolism in Cancer. *Front Oncol*, *8*, 160. https://doi.org/10.3389/fonc.2018.00160

Kullmann, L., & Krahn, M. P. (2018). Controlling the master-upstream regulation of the tumor suppressor LKB1. *Oncogene*, *37*(23), 3045-3057. https://doi.org/10.1038/s41388-018-0145-z

Lamouille, S., Xu, J., & Derynck, R. (2014). Molecular mechanisms of epithelial-mesenchymal transition. *Nat Rev Mol Cell Biol*, *15*(3), 178-196. https://doi.org/10.1038/nrm3758

Lapshyn, H., Bolm, L., Kohler, I., Werner, M., Billmann, F. G., Bausch, D., Hopt, U. T., Makowiec, F., Wittel, U. A., Keck, T., Bronsert, P., & Wellner, U. F. (2017). Histopathological tumor invasion of the mesenterico-portal vein is characterized by aggressive biology and stromal fibroblast activation. *HPB (Oxford)*, *19*(1), 67-74. https://doi.org/10.1016/j.hpb.2016.10.002

Lawlor, R. T., Veronese, N., Nottegar, A., Malleo, G., Smith, L., Demurtas, J., Cheng, L., Wood, L. D., Silvestris, N., Salvia, R., Scarpa, A., & Luchini, C. (2019). Prognostic Role of High-Grade Tumor Budding in Pancreatic Ductal Adenocarcinoma: A Systematic Review and Meta-Analysis with a Focus on Epithelial to Mesenchymal Transition. *Cancers (Basel)*, *11*(1). https://doi.org/10.3390/cancers11010113

Li, D., Tang, H., Hassan, M. M., Holly, E. A., Bracci, P. M., & Silverman, D. T. (2011). Diabetes and risk of pancreatic cancer: a pooled analysis of three large case-control studies. *Cancer Causes Control*, *22*(2), 189-197. https://doi.org/10.1007/s10552-010-9686-3

Li, L., & Li, W. (2015). Epithelial-mesenchymal transition in human cancer: comprehensive reprogramming of metabolism, epigenetics, and differentiation. *Pharmacol Ther*, *150*, 33-46. https://doi.org/10.1016/j.pharmthera.2015.01.004

Liu, D. N., Lv, A., Tian, Z. H., Tian, X. Y., Guan, X. Y., Dong, B., Zhao, M., & Hao, C. Y. (2017). Superior mesenteric artery margin in pancreaticoduodenectomy for pancreatic adenocarcinoma. *Oncotarget*, *8*(5), 7766-7776. https://doi.org/10.18632/oncotarget.13950

Livak, K. J., & Schmittgen, T. D. (2001). Analysis of relative gene expression data using real-time quantitative PCR and the 2(-Delta Delta C(T)) Method. *Methods*, *25*(4), 402-408. https://doi.org/10.1006/meth.2001.1262

Lynch, S. M., Vrieling, A., Lubin, J. H., Kraft, P., Mendelsohn, J. B., Hartge, P., Canzian, F., Steplowski, E., Arslan, A. A., Gross, M., Helzlsouer, K., Jacobs, E. J., LaCroix, A., Petersen, G., Zheng, W., Albanes, D., Amundadottir, L., Bingham, S. A., Boffetta, P., Boutron-Ruault, M. C., Chanock, S. J., Clipp, S., Hoover, R. N., Jacobs, K., Johnson, K. C., Kooperberg, C., Luo, J., Messina, C., Palli, D., Patel, A. V., Riboli, E., Shu, X. O., Rodriguez Suarez, L., Thomas, G., Tjonneland, A., Tobias, G. S., Tong, E., Trichopoulos, D., Virtamo, J., Ye, W., Yu, K., Zeleniuch-Jacquette, A., Bueno-de-Mesquita, H. B., & Stolzenberg-Solomon, R. Z. (2009). Cigarette smoking and pancreatic cancer: a pooled analysis from the pancreatic cancer cohort consortium. *Am J Epidemiol*, *170*(4), 403-413. https://doi.org/10.1093/aje/kwp134

Maisonneuve, P., Amar, S., & Lowenfels, A. B. (2017). Periodontal disease, edentulism, and pancreatic cancer: a meta-analysis. *Ann Oncol*, *28*(5), 985-995. https://doi.org/10.1093/annonc/mdx019

Makohon-Moore, A. P., Zhang, M., Reiter, J. G., Bozic, I., Allen, B., Kundu, D., Chatterjee, K., Wong, F., Jiao, Y., Kohutek, Z. A., Hong, J., Attiyeh, M., Javier, B., Wood, L. D., Hruban, R. H., Nowak, M. A., Papadopoulos, N., Kinzler, K. W., Vogelstein, B., & Iacobuzio-Donahue, C. A. (2017). Limited heterogeneity of known driver gene mutations among the metastases of individual patients with pancreatic cancer. *Nat Genet*, *49*(3), 358-366. https://doi.org/10.1038/ng.3764

Mann, K. M., Ying, H., Juan, J., Jenkins, N. A., & Copeland, N. G. (2016). KRAS-related proteins in pancreatic cancer. *Pharmacol Ther*, *168*, 29-42. https://doi.org/10.1016/j.pharmthera.2016.09.003

Marinho, H. S., Real, C., Cyrne, L., Soares, H., & Antunes, F. (2014). Hydrogen peroxide sensing, signaling and regulation of transcription factors. *Redox Biol*, *2*, 535-562. https://doi.org/10.1016/j.redox.2014.02.006

Marmol, I., Quero, J., Rodriguez-Yoldi, M. J., & Cerrada, E. (2019). Gold as a Possible Alternative to Platinum-Based Chemotherapy for Colon Cancer Treatment. *Cancers (Basel)*, *11*(6). https://doi.org/10.3390/cancers11060780

Martinez-Useros, J., Li, W., Cabeza-Morales, M., & Garcia-Foncillas, J. (2017). Oxidative Stress: A New Target for Pancreatic Cancer Prognosis and Treatment. *J Clin Med*, *6*(3). https://doi.org/10.3390/jcm6030029

Mees, S. T., Mardin, W. A., Wendel, C., Baeumer, N., Willscher, E., Senninger, N., Schleicher, C., Colombo-Benkmann, M., & Haier, J. (2010). EP300--a miRNA-regulated metastasis suppressor gene in ductal adenocarcinomas of the pancreas. *Int J Cancer*, *126*(1), 114-124. https://doi.org/10.1002/ijc.24695

Michaud, D. S., Giovannucci, E., Willett, W. C., Colditz, G. A., Stampfer, M. J., & Fuchs, C. S. (2001). Physical activity, obesity, height, and the risk of pancreatic cancer. *JAMA*, *286*(8), 921-929. https://doi.org/10.1001/jama.286.8.921

Miranda-Vizuete, A., Damdimopoulos, A. E., Pedrajas, J. R., Gustafsson, J. A., & Spyrou, G. (1999). Human mitochondrial thioredoxin reductase cDNA cloning, expression and genomic organization. *Eur J Biochem*, *261*(2), 405-412. https://doi.org/10.1046/j.1432-1327.1999.00286.x

Moffitt, R. A., Marayati, R., Flate, E. L., Volmar, K. E., Loeza, S. G., Hoadley, K. A., Rashid, N. U., Williams, L. A., Eaton, S. C., Chung, A. H., Smyla, J. K., Anderson, J. M., Kim, H. J., Bentrem, D. J., Talamonti, M. S., Iacobuzio-Donahue, C. A., Hollingsworth, M. A., & Yeh, J. J. (2015). Virtual microdissection identifies distinct tumor- and stroma-specific subtypes of pancreatic ductal adenocarcinoma. *Nat Genet*, *47*(10), 1168-1178. https://doi.org/10.1038/ng.3398

Moore, A. R., Rosenberg, S. C., McCormick, F., & Malek, S. (2020). RAS-targeted therapies: is the undruggable drugged? *Nat Rev Drug Discov*, *19*(8), 533-552. https://doi.org/10.1038/s41573-020-0068-6

Mungai, P. T., Waypa, G. B., Jairaman, A., Prakriya, M., Dokic, D., Ball, M. K., & Schumacker, P. T. (2011). Hypoxia triggers AMPK activation through reactive oxygen species-mediated activation of calcium release-activated calcium channels. *Mol Cell Biol*, *31*(17), 3531-3545. https://doi.org/10.1128/MCB.05124-11

Nakamura, H., Bai, J., Nishinaka, Y., Ueda, S., Sasada, T., Ohshio, G., Imamura, M., Takabayashi, A., Yamaoka, Y., & Yodoi, J. (2000). Expression of thioredoxin and glutaredoxin, redox-regulating proteins, in pancreatic cancer. *Cancer Detect Prev*, *24*(1), 53-60. https://www.ncbi.nlm.nih.gov/pubmed/10757123

Nakamura, H., Masutani, H., Tagaya, Y., Yamauchi, A., Inamoto, T., Nanbu, Y., Fujii, S., Ozawa, K., & Yodoi, J. (1992). Expression and growth-promoting effect of adult T-cell leukemia-derived factor. A human thioredoxin homologue in hepatocellular carcinoma. *Cancer*, *69*(8), 2091-2097. https://doi.org/10.1002/1097-0142(19920415)69:8<2091::aid-cncr2820690814>3.0.co;2-x

Nieto, M. A., Huang, R. Y., Jackson, R. A., & Thiery, J. P. (2016). Emt: 2016. *Cell*, *166*(1), 21-45. https://doi.org/10.1016/j.cell.2016.06.028

Olson, S. H., Chou, J. F., Ludwig, E., O'Reilly, E., Allen, P. J., Jarnagin, W. R., Bayuga, S., Simon, J., Gonen, M., Reisacher, W. R., & Kurtz, R. C. (2010). Allergies, obesity, other risk factors and survival from pancreatic cancer. *Int J Cancer*, *127*(10), 2412-2419. https://doi.org/10.1002/ijc.25240

Orth, M., Metzger, P., Gerum, S., Mayerle, J., Schneider, G., Belka, C., Schnurr, M., & Lauber, K. (2019). Pancreatic ductal adenocarcinoma: biological hallmarks,

current status, and future perspectives of combined modality treatment approaches. *Radiat Oncol*, *14*(1), 141. https://doi.org/10.1186/s13014-019-1345-6

Ott, M., Gogvadze, V., Orrenius, S., & Zhivotovsky, B. (2007). Mitochondria, oxidative stress and cell death. *Apoptosis*, *12*(5), 913-922. https://doi.org/10.1007/s10495-007-0756-2

Palamaris, K., Felekouras, E., & Sakellariou, S. (2021). Epithelial to Mesenchymal Transition: Key Regulator of Pancreatic Ductal Adenocarcinoma Progression and Chemoresistance. *Cancers (Basel)*, *13*(21). https://doi.org/10.3390/cancers13215532

Peinado, H., Olmeda, D., & Cano, A. (2007). Snail, Zeb and bHLH factors in tumour progression: an alliance against the epithelial phenotype? *Nat Rev Cancer*, *7*(6), 415-428. https://doi.org/10.1038/nrc2131

Pelucchi, C., Galeone, C., Polesel, J., Manzari, M., Zucchetto, A., Talamini, R., Franceschi, S., Negri, E., & La Vecchia, C. (2014). Smoking and body mass index and survival in pancreatic cancer patients. *Pancreas*, *43*(1), 47-52. https://doi.org/10.1097/MPA.0b013e3182a7c74b

Peng, X., Gimenez-Cassina, A., Petrus, P., Conrad, M., Ryden, M., & Arner, E. S. (2016). Thioredoxin reductase 1 suppresses adipocyte differentiation and insulin responsiveness. *Sci Rep*, *6*, 28080. https://doi.org/10.1038/srep28080

Penugurti, V., Mishra, Y. G., & Manavathi, B. (2022). AMPK: An odyssey of a metabolic regulator, a tumor suppressor, and now a contextual oncogene. *Biochim Biophys Acta Rev Cancer*, *1877*(5), 188785. https://doi.org/10.1016/j.bbcan.2022.188785

Petersen, G. M., Amundadottir, L., Fuchs, C. S., Kraft, P., Stolzenberg-Solomon, R. Z., Jacobs, K. B., Arslan, A. A., Bueno-de-Mesquita, H. B., Gallinger, S., Gross, M.,

Helzlsouer, K., Holly, E. A., Jacobs, E. J., Klein, A. P., LaCroix, A., Li, D., Mandelson, M. T., Olson, S. H., Risch, H. A., Zheng, W., Albanes, D., Bamlet, W. R., Berg, C. D., Boutron-Ruault, M. C., Buring, J. E., Bracci, P. M., Canzian, F., Clipp, S., Cotterchio, M., de Andrade, M., Duell, E. J., Gaziano, J. M., Giovannucci, E. L., Goggins, M., Hallmans, G., Hankinson, S. E., Hassan, M., Howard, B., Hunter, D. J., Hutchinson, A., Jenab, M., Kaaks, R., Kooperberg, C., Krogh, V., Kurtz, R. C., Lynch, S. M., McWilliams, R. R., Mendelsohn, J. B., Michaud, D. S., Parikh, H., Patel, A. V., Peeters, P. H., Rajkovic, A., Riboli, E., Rodriguez, L., Seminara, D., Shu, X. O., Thomas, G., Tjonneland, A., Tobias, G. S., Trichopoulos, D., Van Den Eeden, S. K., Virtamo, J., Wactawski-Wende, J., Wang, Z., Wolpin, B. M., Yu, H., Yu, K., Zeleniuch-Jacquotte, A., Fraumeni, J. F., Jr., Hoover, R. N., Hartge, P., & Chanock, S. J. (2010). A genome-wide association study identifies pancreatic cancer susceptibility loci on chromosomes 13q22.1, 1q32.1 and 5p15.33. *Nat Genet*, *42*(3), 224-228. https://doi.org/10.1038/ng.522

Pihlak, R., Valle, J. W., & McNamara, M. G. (2017). Germline mutations in pancreatic cancer and potential new therapeutic options. *Oncotarget*, *8*(42), 73240-73257. https://doi.org/10.18632/oncotarget.17291

Ponnusamy, L., Natarajan, S. R., Thangaraj, K., & Manoharan, R. (2020). Therapeutic aspects of AMPK in breast cancer: Progress, challenges, and future directions. *Biochim Biophys Acta Rev Cancer*, *1874*(1), 188379. https://doi.org/10.1016/j.bbcan.2020.188379

Poruk, K. E., Firpo, M. A., Adler, D. G., & Mulvihill, S. J. (2013). Screening for pancreatic cancer: why, how, and who? *Ann Surg*, *257*(1), 17-26. https://doi.org/10.1097/SLA.0b013e31825ffbfb

Purohit, V., Simeone, D. M., & Lyssiotis, C. A. (2019). Metabolic Regulation of Redox Balance in Cancer. *Cancers (Basel)*, *11*(7). https://doi.org/10.3390/cancers11070955

Quante, A. S., Ming, C., Rottmann, M., Engel, J., Boeck, S., Heinemann, V., Westphalen, C. B., & Strauch, K. (2016). Projections of cancer incidence and cancer-related deaths in Germany by 2020 and 2030. *Cancer Med*, *5*(9), 2649-2656. https://doi.org/10.1002/cam4.767

Rabilloud, T., Heller, M., Rigobello, M. P., Bindoli, A., Aebersold, R., & Lunardi, J. (2001). The mitochondrial antioxidant defence system and its response to oxidative stress. *Proteomics*, *1*(9), 1105-1110. https://doi.org/10.1002/1615-9861(200109)1:9<1105::AID-PROT1105>3.0.CO;2-M

Rabinovitch, R. C., Samborska, B., Faubert, B., Ma, E. H., Gravel, S. P., Andrzejewski, S., Raissi, T. C., Pause, A., St-Pierre, J., & Jones, R. G. (2017). AMPK Maintains Cellular Metabolic Homeostasis through Regulation of Mitochondrial Reactive Oxygen Species. *Cell Rep*, *21*(1), 1-9. https://doi.org/10.1016/j.celrep.2017.09.026

Rahn, S., Zimmermann, V., Viol, F., Knaack, H., Stemmer, K., Peters, L., Lenk, L., Ungefroren, H., Saur, D., Schafer, H., Helm, O., & Sebens, S. (2018). Diabetes as risk factor for pancreatic cancer: Hyperglycemia promotes epithelial-mesenchymal-transition and stem cell properties in pancreatic ductal epithelial cells. *Cancer Lett*, *415*, 129-150. https://doi.org/10.1016/j.canlet.2017.12.004

Reczek, C. R., Birsoy, K., Kong, H., Martinez-Reyes, I., Wang, T., Gao, P., Sabatini, D. M., & Chandel, N. S. (2017). A CRISPR screen identifies a pathway required for paraquat-induced cell death. *Nat Chem Biol*, *13*(12), 1274-1279. https://doi.org/10.1038/nchembio.2499

Redza-Dutordoir, M., & Averill-Bates, D. A. (2016). Activation of apoptosis signalling pathways by reactive oxygen species. *Biochim Biophys Acta*, *1863*(12), 2977-2992. https://doi.org/10.1016/j.bbamcr.2016.09.012

Rhim, A. D., Mirek, E. T., Aiello, N. M., Maitra, A., Bailey, J. M., McAllister, F., Reichert, M., Beatty, G. L., Rustgi, A. K., Vonderheide, R. H., Leach, S. D., & Stanger, B. Z. (2012). EMT and dissemination precede pancreatic tumor formation. *Cell*, *148*(1-2), 349-361. https://doi.org/10.1016/j.cell.2011.11.025

Rigobello, M. P., Folda, A., Baldoin, M. C., Scutari, G., & Bindoli, A. (2005). Effect of auranofin on the mitochondrial generation of hydrogen peroxide. Role of thioredoxin reductase. *Free Radic Res*, *39*(7), 687-695. https://doi.org/10.1080/10715760500135391

Riquelme, E., Zhang, Y., Zhang, L., Montiel, M., Zoltan, M., Dong, W., Quesada, P., Sahin, I., Chandra, V., San Lucas, A., Scheet, P., Xu, H., Hanash, S. M., Feng, L., Burks, J. K., Do, K. A., Peterson, C. B., Nejman, D., Tzeng, C. D., Kim, M. P., Sears, C. L., Ajami, N., Petrosino, J., Wood, L. D., Maitra, A., Straussman, R., Katz, M., White, J. R., Jenq, R., Wargo, J., & McAllister, F. (2019). Tumor Microbiome Diversity and Composition Influence Pancreatic Cancer Outcomes. *Cell*, *178*(4), 795-806 e712. https://doi.org/10.1016/j.cell.2019.07.008

Rozengurt, E., & Eibl, G. (2021). Crosstalk between KRAS, SRC and YAP Signaling in Pancreatic Cancer: Interactions Leading to Aggressive Disease and Drug Resistance. *Cancers (Basel)*, *13*(20). https://doi.org/10.3390/cancers13205126

Scaglia, N., Tyekucheva, S., Zadra, G., Photopoulos, C., & Loda, M. (2014). De novo fatty acid synthesis at the mitotic exit is required to complete cellular division. *Cell Cycle*, *13*(5), 859-868. https://doi.org/10.4161/cc.27767

Shaw, R. J., Kosmatka, M., Bardeesy, N., Hurley, R. L., Witters, L. A., DePinho, R. A., & Cantley, L. C. (2004). The tumor suppressor LKB1 kinase directly activates

AMP-activated kinase and regulates apoptosis in response to energy stress. *Proc Natl Acad Sci U S A*, *101*(10), 3329-3335. https://doi.org/10.1073/pnas.0308061100

Shen, C. H., Yuan, P., Perez-Lorenzo, R., Zhang, Y., Lee, S. X., Ou, Y., Asara, J. M., Cantley, L. C., & Zheng, B. (2013). Phosphorylation of BRAF by AMPK impairs BRAF-KSR1 association and cell proliferation. *Mol Cell*, *52*(2), 161-172. https://doi.org/10.1016/j.molcel.2013.08.044

Shi, D., Guo, L., Sun, X., Shang, M., Meng, D., Zhou, X., Liu, X., Zhao, Y., & Li, J. (2020). UTMD inhibit EMT of breast cancer through the ROS/miR-200c/ZEB1 axis. *Sci Rep*, *10*(1), 6657. https://doi.org/10.1038/s41598-020-63653-w

Shook, D., & Keller, R. (2003). Mechanisms, mechanics and function of epithelial-mesenchymal transitions in early development. *Mech Dev*, *120*(11), 1351-1383. https://doi.org/10.1016/j.mod.2003.06.005

Siegel, R., Ma, J., Zou, Z., & Jemal, A. (2014). Cancer statistics, 2014. *CA Cancer J Clin*, *64*(1), 9-29. https://doi.org/10.3322/caac.21208

Siegel, R. L., Miller, K. D., & Jemal, A. (2018). Cancer statistics, 2018. *CA Cancer J Clin*, *68*(1), 7-30. https://doi.org/10.3322/caac.21442

Siegel, R. L., Miller, K. D., & Jemal, A. (2020). Cancer statistics, 2020. *CA Cancer J Clin*, *70*(1), 7-30. https://doi.org/10.3322/caac.21590

Sies, H. (2015). Oxidative stress: a concept in redox biology and medicine. *Redox Biol*, *4*, 180-183. https://doi.org/10.1016/j.redox.2015.01.002

Soderberg, A., Sahaf, B., & Rosen, A. (2000). Thioredoxin reductase, a redox-active selenoprotein, is secreted by normal and neoplastic cells: presence in human plasma. *Cancer Res*, *60*(8), 2281-2289. https://www.ncbi.nlm.nih.gov/pubmed/10786696

St-Pierre, J., Drori, S., Uldry, M., Silvaggi, J. M., Rhee, J., Jager, S., Handschin, C., Zheng, K., Lin, J., Yang, W., Simon, D. K., Bachoo, R., & Spiegelman, B. M. (2006). Suppression of reactive oxygen species and neurodegeneration by the PGC-1 transcriptional coactivators. *Cell*, *127*(2), 397-408. https://doi.org/10.1016/j.cell.2006.09.024

Stafford, W. C., Peng, X., Olofsson, M. H., Zhang, X., Luci, D. K., Lu, L., Cheng, Q., Tresaugues, L., Dexheimer, T. S., Coussens, N. P., Augsten, M., Ahlzen, H. M., Orwar, O., Ostman, A., Stone-Elander, S., Maloney, D. J., Jadhav, A., Simeonov, A., Linder, S., & Arner, E. S. J. (2018). Irreversible inhibition of cytosolic thioredoxin reductase 1 as a mechanistic basis for anticancer therapy. *Sci Transl Med*, *10*(428). https://doi.org/10.1126/scitranslmed.aaf7444

Sun, Q. A., Zappacosta, F., Factor, V. M., Wirth, P. J., Hatfield, D. L., & Gladyshev, V. N. (2001). Heterogeneity within animal thioredoxin reductases. Evidence for alternative first exon splicing. *J Biol Chem*, *276*(5), 3106-3114. https://doi.org/10.1074/jbc.M004750200

Suter, M., Riek, U., Tuerk, R., Schlattner, U., Wallimann, T., & Neumann, D. (2006). Dissecting the role of 5'-AMP for allosteric stimulation, activation, and deactivation of AMP-activated protein kinase. *J Biol Chem*, *281*(43), 32207-32216. https://doi.org/10.1074/jbc.M606357200

Takano, S., Reichert, M., Bakir, B., Das, K. K., Nishida, T., Miyazaki, M., Heeg, S., Collins, M. A., Marchand, B., Hicks, P. D., Maitra, A., & Rustgi, A. K. (2016). Prrx1 isoform switching regulates pancreatic cancer invasion and metastatic colonization. *Genes Dev*, *30*(2), 233-247. https://doi.org/10.1101/gad.263327.115

Walhout, A. J., Temple, G. F., Brasch, M. A., Hartley, J. L., Lorson, M. A., van den Heuvel, S., & Vidal, M. (2000). GATEWAY recombinational cloning: application

to the cloning of large numbers of open reading frames or ORFeomes. *Methods Enzymol*, *328*, 575-592. https://doi.org/10.1016/s0076-6879(00)28419-x

Wang, L., Yang, Z., Fu, J., Yin, H., Xiong, K., Tan, Q., Jin, H., Li, J., Wang, T., Tang, W., Yin, J., Cai, G., Liu, M., Kehr, S., Becker, K., & Zeng, H. (2012). Ethaselen: a potent mammalian thioredoxin reductase 1 inhibitor and novel organoselenium anticancer agent. *Free Radic Biol Med*, *52*(5), 898-908. https://doi.org/10.1016/j.freeradbiomed.2011.11.034

Wang, S., Huang, S., & Sun, Y. L. (2017). Epithelial-Mesenchymal Transition in Pancreatic Cancer: A Review. *Biomed Res Int*, *2017*, 2646148. https://doi.org/10.1155/2017/2646148

Wartenberg, M., Cibin, S., Zlobec, I., Vassella, E., Eppenberger-Castori, S., Terracciano, L., Eichmann, M. D., Worni, M., Gloor, B., Perren, A., & Karamitopoulou, E. (2018). Integrated Genomic and Immunophenotypic Classification of Pancreatic Cancer Reveals Three Distinct Subtypes with Prognostic/Predictive Significance. *Clin Cancer Res*, *24*(18), 4444-4454. https://doi.org/10.1158/1078-0432.CCR-17-3401

Watson, J. (2013). Oxidants, antioxidants and the current incurability of metastatic cancers. *Open Biol*, *3*(1), 120144. https://doi.org/10.1098/rsob.120144

Wisnoski, N. C., Townsend, C. M., Jr., Nealon, W. H., Freeman, J. L., & Riall, T. S. (2008). 672 patients with acinar cell carcinoma of the pancreas: a population-based comparison to pancreatic adenocarcinoma. *Surgery*, *144*(2), 141-148. https://doi.org/10.1016/j.surg.2008.03.006

Wood, L. D., & Hruban, R. H. (2012). Pathology and molecular genetics of pancreatic neoplasms. *Cancer J*, *18*(6), 492-501. https://doi.org/10.1097/PPO.0b013e31827459b6

Woods, A., Dickerson, K., Heath, R., Hong, S. P., Momcilovic, M., Johnstone, S. R., Carlson, M., & Carling, D. (2005). Ca2+/calmodulin-dependent protein kinase kinase-beta acts upstream of AMP-activated protein kinase in mammalian cells. *Cell Metab*, *2*(1), 21-33. https://doi.org/10.1016/j.cmet.2005.06.005

Woods, A., Johnstone, S. R., Dickerson, K., Leiper, F. C., Fryer, L. G., Neumann, D., Schlattner, U., Wallimann, T., Carlson, M., & Carling, D. (2003). LKB1 is the upstream kinase in the AMP-activated protein kinase cascade. *Curr Biol*, *13*(22), 2004-2008. https://doi.org/10.1016/j.cub.2003.10.031

Xiao, G. G., Wang, M., Li, N., Loo, J. A., & Nel, A. E. (2003). Use of proteomics to demonstrate a hierarchical oxidative stress response to diesel exhaust particle chemicals in a macrophage cell line. *J Biol Chem*, *278*(50), 50781-50790. https://doi.org/10.1074/jbc.M306423200

Yadav, D., & Lowenfels, A. B. (2013). The epidemiology of pancreatitis and pancreatic cancer. *Gastroenterology*, *144*(6), 1252-1261. https://doi.org/10.1053/j.gastro.2013.01.068

Yamada, S., Fuchs, B. C., Fujii, T., Shimoyama, Y., Sugimoto, H., Nomoto, S., Takeda, S., Tanabe, K. K., Kodera, Y., & Nakao, A. (2013). Epithelial-to-mesenchymal transition predicts prognosis of pancreatic cancer. *Surgery*, *154*(5), 946-954. https://doi.org/10.1016/j.surg.2013.05.004

Yan, X., Zhang, X., Wang, L., Zhang, R., Pu, X., Wu, S., Li, L., Tong, P., Wang, J., Meng, Q. H., Jensen, V. B., Girard, L., Minna, J. D., Roth, J. A., Swisher, S. G., Heymach, J. V., & Fang, B. (2019). Inhibition of Thioredoxin/Thioredoxin Reductase Induces Synthetic Lethality in Lung Cancers with Compromised Glutathione Homeostasis. *Cancer Res*, *79*(1), 125-132. https://doi.org/10.1158/0008-5472.CAN-18-1938

Yang, D., Guo, Q., Liang, Y., Zhao, Y., Tian, X., Ye, Y., Tian, J., Wu, T., & Lu, N. (2020). Wogonin induces cellular senescence in breast cancer via suppressing TXNRD2 expression. *Arch Toxicol*, *94*(10), 3433-3447. https://doi.org/10.1007/s00204-020-02842-y

Zadra, G., Batista, J. L., & Loda, M. (2015). Dissecting the Dual Role of AMPK in Cancer: From Experimental to Human Studies. *Mol Cancer Res*, *13*(7), 1059-1072. https://doi.org/10.1158/1541-7786.MCR-15-0068

Zhang, B., Zhang, J., Peng, S., Liu, R., Li, X., Hou, Y., Han, X., & Fang, J. (2017). Thioredoxin reductase inhibitors: a patent review. *Expert Opin Ther Pat*, *27*(5), 547-556. https://doi.org/10.1080/13543776.2017.1272576

Zhang, H., Go, Y. M., & Jones, D. P. (2007). Mitochondrial thioredoxin-2/peroxiredoxin-3 system functions in parallel with mitochondrial GSH system in protection against oxidative stress. *Arch Biochem Biophys*, *465*(1), 119-126. https://doi.org/10.1016/j.abb.2007.05.001

Zhang, S., Wang, C., Huang, H., Jiang, Q., Zhao, D., Tian, Y., Ma, J., Yuan, W., Sun, Y., Che, X., Zhang, J., Chen, H., Zhao, Y., Chu, Y., Zhang, Y., & Chen, Y. (2017). Effects of alcohol drinking and smoking on pancreatic ductal adenocarcinoma mortality: A retrospective cohort study consisting of 1783 patients. *Sci Rep*, *7*(1), 9572. https://doi.org/10.1038/s41598-017-08794-1

Zhao, Y., Hu, X., Liu, Y., Dong, S., Wen, Z., He, W., Zhang, S., Huang, Q., & Shi, M. (2017). ROS signaling under metabolic stress: cross-talk between AMPK and AKT pathway. *Mol Cancer*, *16*(1), 79. https://doi.org/10.1186/s12943-017-0648-1

ACKNOWLEDGEMENTS

First of all, I want to express my deep gratitude to my professor, prof Roland M Schmid for letting me be a member of the team and giving the access to the laboratory and research facilities. Without his support, it would not be possible for me to conduct this research and finish my study.

I also want to thank my mentor, Dr. Henrik Einwächter, for always being there when I needed his support, reviewing my progress constantly, and guiding me through my research.

I would like to thank my colleague, Thorsten Neuß. His assisting with the practical, technical and theoretical aspects of my research over the last 4 years, is immeasurable. He helped with the most complicated questions and spent hours with me improving my work.

Furthermore, many thanks to all my co-workers, Sankaranarayanan Ramasubramanian, Bailing Li, Leeanne Mundle, Nirav Chhabra, Min-Chun Chen,Judit Desztics, Ali Altaee, Anke Bettenbrock, Anja Motz, Mathilde Neuhofer, for their editing help, late-night feedback sessions, and moral support. Especially thanks to Thorsten, Sankar, Nirav and Leeanne for spending time revising my thesis manuscript. Your comments have been very valuable and helpful.,

Last but not least, my warm and heartfelt thanks go to my family. Their belief in me has kept my spirits and motivation high during this process. Without that support, this thesis would not have been possible.